ELECTRICAL

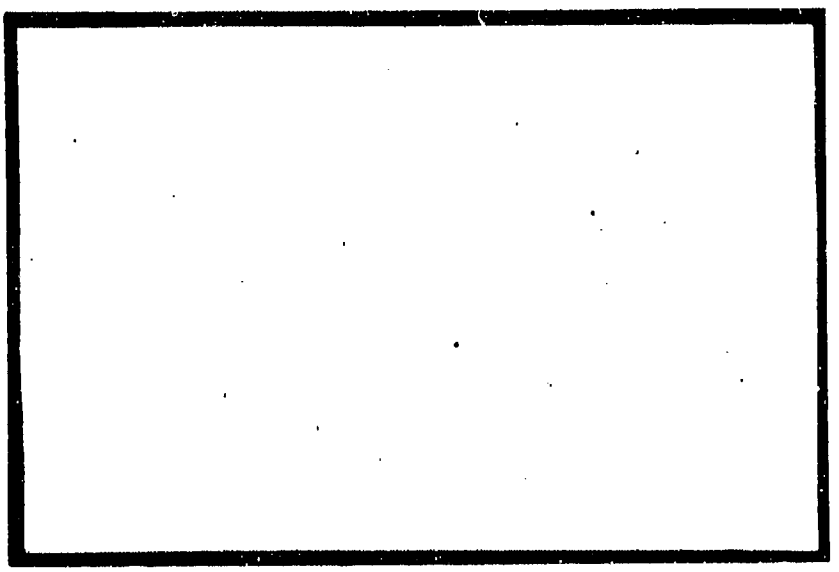

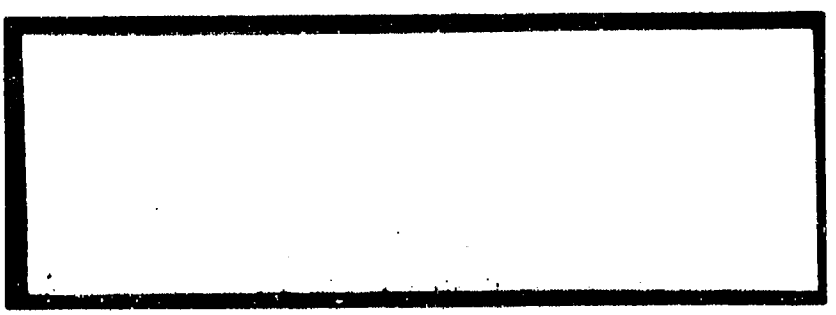

ENGINEERING EXPERIMENT STATION

AUBURN UNIVERSITY

AUBURN, ALABAMA

FINAL REPORT PART II

TRANSIENT ANALYSIS OF A FINITE LENGTH CYLINDRICAL SCATTERER NEAR IMPERFECTLY CONDUCTING GROUND

Prepared by

T.H. Shumpert
Project Leader

15 November 1977

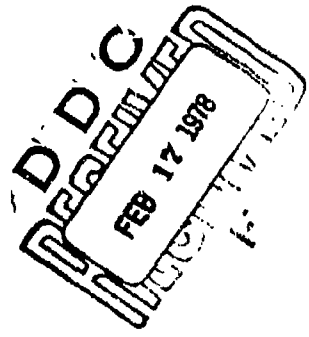

Contract No. F44620-76-C-0054

Air Force Office of Scientific Research

Bolling AFB, D.C. 20332

UNCLASSIFIED

SECURITY CLASSIFICATION OF THIS PAGE (When Data Entered)

REPORT DOCUMENTATION PAGE

READ INSTRUCTIONS BEFORE COMPLETING FORM

1. REPORT NUMBER: AFOSR-TR-78-1181-Pt-2	2. GOVT ACCESSION NO. / 3. RECIPIENT'S CATALOG NUMBER
4. TITLE (and Subtitle): TRANSIENT ANALYSIS OF A FINITE LENGTH CYLINDRICAL SCATTERER VERY NEAR A PERFECTLY CONDUCTING GROUND. Part II.	5. TYPE OF REPORT & PERIOD COVERED: Final Reptg Part II
	6. PERFORMING ORG. REPORT NUMBER
7. AUTHOR(s): T. H. Shumpert	8. CONTRACT OR GRANT NUMBER(s): F44620-76-C-0054
9. PERFORMING ORGANIZATION NAME AND ADDRESS: Engineering Experiment Station, Auburn University, Aubur, Alabama	10. PROGRAM ELEMENT, PROJECT, TASK AREA & WORK UNIT NUMBERS: 61102F, 2311/B3
11. CONTROLLING OFFICE NAME AND ADDRESS: AFOSR/NP, Bolling AFB, Bldg.#410, Wash DC 20332	12. REPORT DATE: Nov 1977 / 13. NUMBER OF PAGES: 42 pp
14. MONITORING AGENCY NAME & ADDRESS (if different from Controlling Office)	15. SECURITY CLASS. (of this report): Unclassified / 15a. DECLASSIFICATION/DOWNGRADING SCHEDULE

16. DISTRIBUTION STATEMENT (of this Report)

Approved for public release; distribution unlimited.

17. DISTRIBUTION STATEMENT (of the abstract entered in Block 20, if different from Report)

18. SUPPLEMENTARY NOTES

19. KEY WORDS (Continue on reverse side if necessary and identify by block number)

20. ABSTRACT (Continue on reverse side if necessary and identify by block number)

In attempting to model and predict the magnitude of the surface currents induced on aircraft in the ground-alert mode, it is necessary to examine the effects of the near proximity of the earth's surface. For thin cylindrical scatterers sufficiently far removed (several wavelengths) from the surface, these effects may be taken into account with filamentary currents on the scatterer and its image. However, if the scatterer is moved very near (a fraction of a wavelength) to the ground, the assumption of filamentary currents is invalidated. In this note a transmission line mode approximation is used to model the circumferential

DD FORM 1 JAN 73 1473 EDITION OF 1 NOV 65 IS OBSOLETE

UNCLASSIFIED

SECURITY CLASSIFICATION OF THIS PAGE (When Data Entered)

AD A052952

variations of the surface current induced on a finite length cylindrical scatterer very near a perfect ground. This solution is compared to previous solutions based on filamentary currents. The results give clear indications as to when the more sophisticated approach should be used to obtain valid solutions to the scattering problems of this type.

FOREWORD

This report is Part II of the Final Technical Report of a study being conducted by the Electrical Engineering Department under the auspices of the Engineering Experiment Station of Auburn University. This technical report is submitted toward fulfillment of the requirements prescribed in AFOSR Contract F44620-76-C-0054.

TABLE OF CONTENTS

I. INTRODUCTION

Numerous investigators have studied the electromagnetic interactions of thin cylinders over a perfectly conducting ground plane illuminated by a distant source [1-6]. There have also been numerous studies of currents induced on infinite cylinders or thin wires near a finitely conducting ground plane [7-9]. In this study a perfectly conducting cylinder of finite length near a finitely conducting ground plane is treated by the Singularity Expansion Method (SEM).

A Pocklington type integro-differential equation is formulated for the current induced on the thin cylinder and its image where the current on the image is related to the current on the object by the ratio of the complex reflection coefficient for the appropriate angle of incidence and polarization involved. In a recent study by Sarkar and Strait [10] it was shown that the above method, termed "reflection method" gave results in the real frequency domain within 10% of the exact Somerfeld formulation for a horizontal electric dipole as long as the dipole was at least $(0.25/\sqrt{\epsilon})\lambda$ from the ground plane. The advantages of the reflection method are speed of computation and interpretation of results.

Using this "reflection method" in the integro-differential equation, this study determines some of the effects of ground conductivity and permittivity upon the natural resonances and natural modes of a thin finite length cylindrical scatterer above a lossy half space. These effects are presented in terms of a family of trajectories in the complex

frequency plane as a function of the electrical and geometrical parameters which define the problem.

I. THEORY

DERIVATION OF INTEGRAL EQUATIONS

In Figure 2-1 an infinitely thin-walled, perfectly conducting, right circular cylinder is shown. As indicated the cylinder is of length L, radius a, and height h above an infinite, finitely conducting ground plane. The system, consisting of the cylinder, ground plane, and incident field of electromagnetic radiation is defined in terms of a combined cartesian and cylindrical coordinate system. The incident electromagnetic field propagates in a general direction described by the angle θ with respect to the z-axis. The current induced on the cylinder by the incident wave is to be determined.

Solution of the above defined problem may be greatly facilitated by the use of image and reflection theory. Applying image theory, the cylinder, incident TEM plane wave, and finitely conducting ground plane are to be replaced by the object cylinder, the image cylinder, and two free space TEM plane waves as shown in Figure 2-2. Reflection theory can be used to show that the currents on the image are related to the currents on the object by the ratio of the complex-reflection coefficient for the appropriate angle of incidence and polarization of the incident field [11-14]. The reflection method cannot be expected to give an exact solution as the cylinder approaches the ground plane [10], [14-16].

Two coordinate systems are defined by Figure 2-3, the object and the image coordinate system indicated by the subscripts "0" and "1"

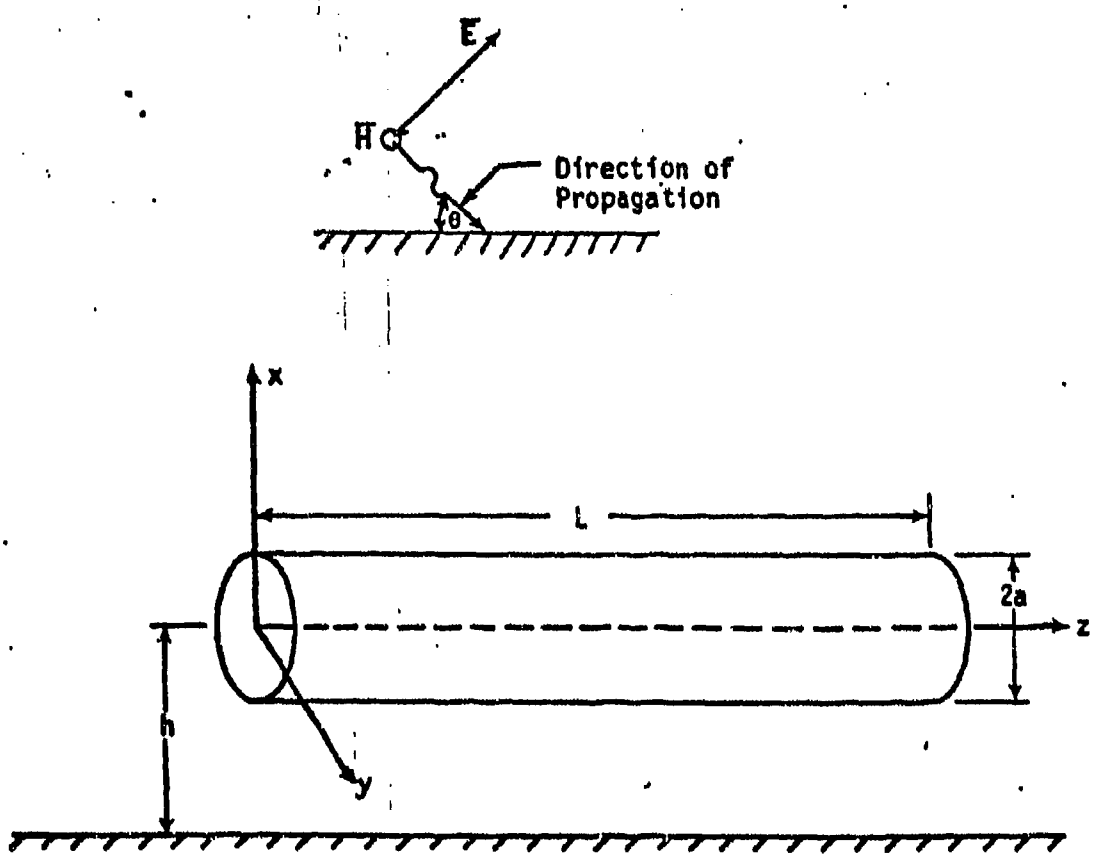

Figure 2-1. Finite Length, Right-Circular Cylinder Near and Parallel to Imperfect Ground Plane, with incident electromagnetic field.

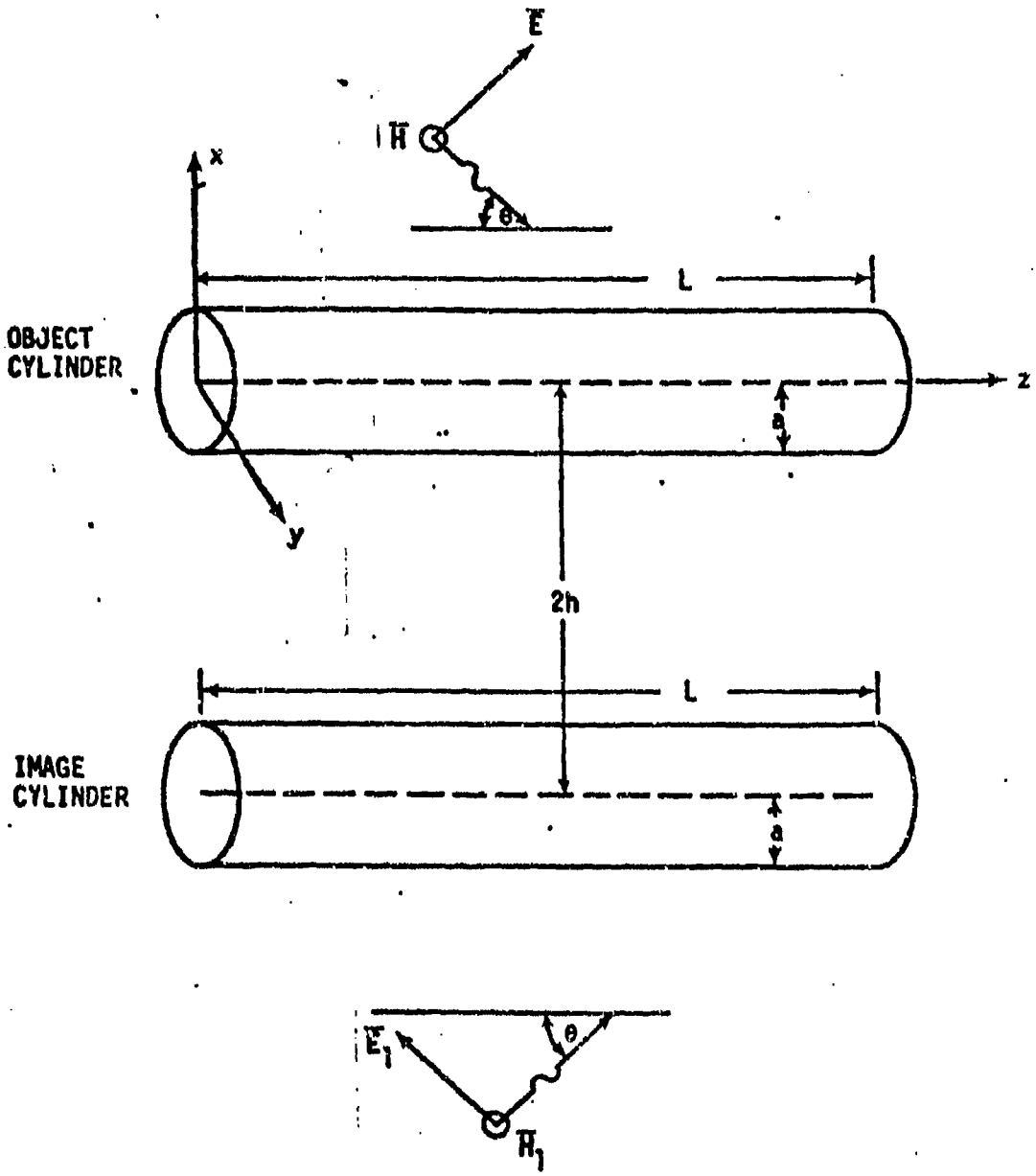

Figure 2-2. Equivalent Image Theory Problem

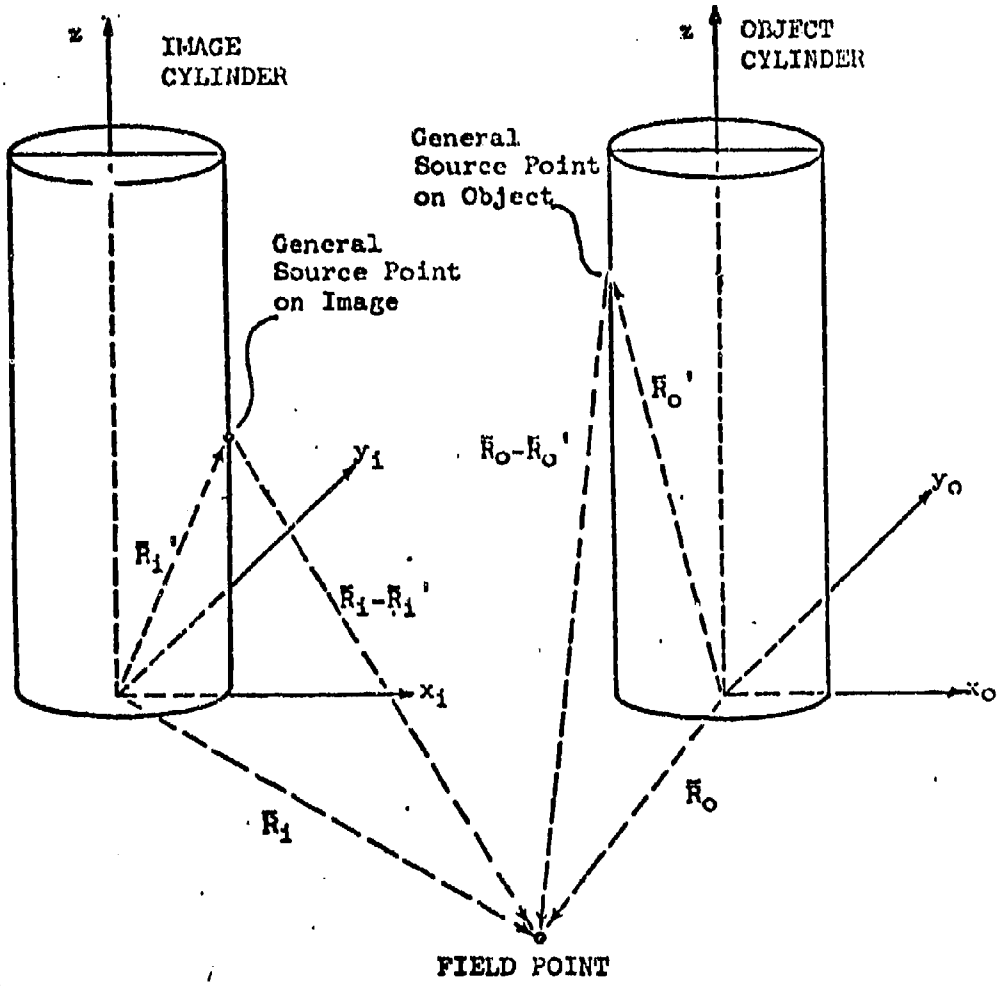

Figure 2-3 General Source and Field Points

respectively. Note that since the cylinders are identical and parallel, z_0 and z_i axes are not necessary. Let the "incident field" be defined as the field plus its reflection from the ground plane. The surface currents induced on the object and its image are considered as source currents radiating in free space [7]. The free space Green's functions may be used to compute the scattered field at an arbitrary field point.

In terms of the geometry as defined by Figure 2-3, appropriate magnetic vector potentials for the object and image are:

$\bar{A}_0(\bar{R}_0)$ = magnetic vector potential of the object in object coordinates

$\bar{A}_i(\bar{R}_i)$ = magnetic vector potential of the image in image coordinates

$\bar{R}_0$ = general field point in space measured from the object coordinate system

$\bar{R}_i$ = same general field point in terms of the image coordinates

$\bar{R}_0'$ = a general source point on the object cylinder with respect to its coordinate system

$\bar{R}_i'$ = a general source point on the image cylinder with respect to its coordinate system

The magnetic vector potential of the object is expressed as

$$\bar{A}_0(\bar{R}_0) = \frac{\mu_0}{4\pi} \int_{s_0'} \bar{K}_0(\bar{R}_0')G_0(\bar{R}_0;\bar{R}_0')ds_0'. \qquad (2\text{-}1)$$

Primed coordinates indicate source points, unprimed coordinates field points;

$G_0(\bar{R}_0;\bar{R}_0')$ = free space Green's function in object coordinates

$\bar{K}_0(\bar{R}_0')$ = surface current density radiating in free space.

In general the free space Green's function has the form

$$G_0(\bar{R}_0;\bar{R}_0') = \frac{\epsilon^{-\gamma|\bar{R}_0 - \bar{R}_0'|}}{|\bar{R}_0 - \bar{R}_0'|} \tag{2-2}$$

The temporal variation ϵ^{st} has been suppressed, where

$$s = \sigma + j\omega, \tag{2-3}$$

The complex frequency variable, with

$$\gamma = s/c \tag{2-4}$$

c = the speed of light in free space.

By the superposition of a cylindrical coordinate system on the cartesian coordinate system of Figure 2-3, the following may be shown:

$$|\bar{R}_0 - \bar{R}_0'| = [\rho_0^2 + \rho_0'^2 - 2\rho_0\rho_0'\cos(\phi_0 - \phi_0') + (z - z')^2]^{\frac{1}{2}} \tag{2-5}$$

where, $\rho_0' = a$, a the radius of the cylinder. Therefore,

$$\bar{A}_0(\bar{R}_0) = \bar{A}_0(\rho_0,\phi_0,z) = \frac{\mu_0}{4\pi} \int_0^L \int_0^{2\pi} \bar{K}_0(\rho_0',\phi_0',z') \cdot$$

$$G_0(\rho_0,\phi_0,z;\rho_0',\phi_0',z')ad\phi_0'dz' \qquad (2\text{-}6)$$

Reduces to

$$\bar{A}_0(\rho_0,\phi_0,z) = \frac{\mu_0}{4\pi} \int_0^L \int_0^{2\pi} \bar{K}_0(\phi_0',z') \frac{\varepsilon^{-\gamma R_1}}{R_1} ad\phi_0'dz' \qquad (2\text{-}7)$$

where

$$R_1 = \left\{\rho_0^2 + a^2 - 2\rho_0 a \cos(\phi_0 - \phi_0') + z - z')^2\right\}^{\frac{1}{2}}. \qquad (2\text{-}8)$$

Assuming no circumferential current components,

$$\bar{K}_0(\phi_0',z') = K_0(\phi_0',z')\hat{a}_z, \qquad (2\text{-}9)$$

Equation (2-7) reduces to

$$A_{0_z}(\rho_0,\phi_0,z) = \frac{\mu_0}{4\pi} \int_0^L \int_0^{2\pi} K_0(\phi_0',z') \frac{\varepsilon^{-\gamma R_1}}{R_1} ad\phi_0'dz'. \qquad (2\text{-}10)$$

A similar process yields

$$A_{1_z}(\rho_1,\phi_1,z) = \frac{\mu_0}{4\pi} \int_0^L \int_0^{2\pi} K_1(\phi_1',z') \frac{\varepsilon^{-\gamma R_2}}{R_2} ad\phi_1'dz', \qquad (2\text{-}11)$$

where

$$R_2 = |\bar{R}_1 - \bar{R}_1'| = [\rho_1^2 + a^2 - 2\rho_1 a \cos(\phi_1 - \phi_1') + (z - z')^2]^{\frac{1}{2}} \tag{2-12}$$

The circumferential variations of the axial current on an infinitely long cylinder over a perfectly conducting ground plane in a static mode has been derived by Taylor [17]. Using Taylor's equation,

$$\bar{K}_0(\phi_0', z) = \frac{I_0(z')}{2\pi a} f_0(\phi_0')\hat{a}_z, \tag{2-13}$$

where

$$f_0(\phi_0') = \frac{[1 - (a/h)^2]^{\frac{1}{2}}}{1 + (a/h)\cos\phi_0'} \tag{2-14}$$

$I_0(z')$ = axial variation of object surface current.

As h becomes large, the circumferential variation of the axial current becomes uniform and thus (2-14) reduces to

$$\bar{K}_0(\phi_0', z') = \frac{I_0(z')}{2\pi a} \hat{a}_z, \tag{2-15}$$

similarly

$$\bar{K}_1(\phi_1', z') = \frac{I_1(z')}{2\pi a} \hat{a}_z, \tag{2-16}$$

The magnetic vector potentials may now be expressed as

$$A_{0z}(\rho_0, \phi_0, z) = \frac{\mu_0}{4\pi} \int_0^L \int_0^{2\pi} \frac{I_0(z')}{2\pi a} \frac{\varepsilon^{-\gamma R_1}}{R_1} a\, d\phi_0' dz' \tag{2-17}$$

$$A_{iz}(\rho_i,\phi_i,z) = \frac{\mu_0}{4\pi} \int_0^L \int_0^{2\pi} \frac{I_i(z')}{2\pi a} \frac{\epsilon^{-\gamma R_2}}{R_2} a d\phi_i' dz'. \qquad (2\text{-}18)$$

Let the general field point of Figure 2-3 be located on the object cylinder. With this restriction the distance R_2 may be calculated in terms of the object coordinate system; see Figure 2-4. From the law of sines,

$$\rho_i \sin \phi_i = a \sin \alpha = a \sin \phi_0 \qquad (2\text{-}19)$$

and from the law of cosines,

$$\rho_i^2 = a^2 + 4h^2 + 4ah \cos \phi_0 \qquad (2\text{-}20)$$

Thus when A_i is evaluated on the object surface,

$$\rho_i = [a^2 + 4h^2 + 4ah \cos \phi_0]^{\frac{1}{2}} \qquad (2\text{-}21)$$

and

$$\phi_i = \sin^{-1}\left[\frac{a \sin \phi_0}{[a^2 + 4h^2 + 4ah \cos \phi_0]^{\frac{1}{2}}}\right] . \qquad (2\text{-}22)$$

Note when $\bar{A}_C$ is evaluated on the surface of the object

$$\rho_0 = a. \qquad (2\text{-}23)$$

With the field point on the object cylinder (2-17) and (2-18) may be written as

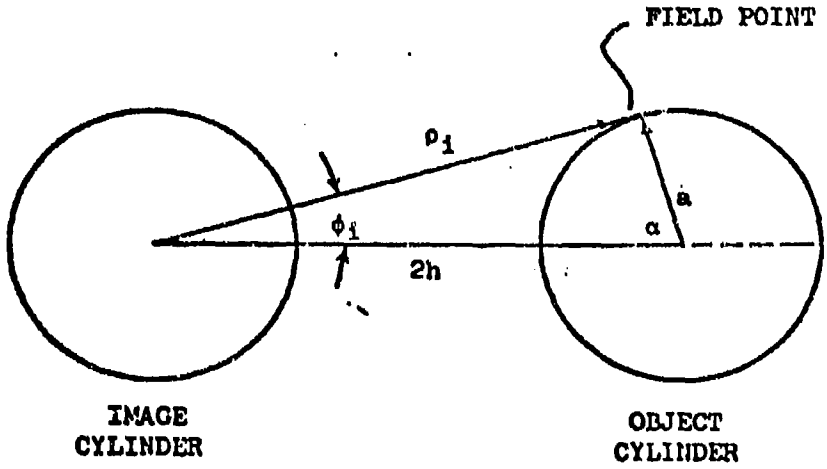

Figure 2-4. Field Point on the Object Surface

$$A_{0z}(\phi_0,z) = \frac{\mu_0}{4\pi} \int_0^L \int_0^{2\pi} \frac{I_0(z')}{2\pi a} \frac{\epsilon^{-\gamma R_1}}{R_1} a d\phi_0' dz' \qquad (2\text{-}24)$$

$$R_1 = [2a^2 - 2a^2\cos(\phi_0 - \phi_0') + (z - z')^2]^{\frac{1}{2}} \qquad (2\text{-}25)$$

$$A_{1z}(\phi_0,z) = \frac{\mu_0}{4\pi} \int_0^L \int_0^{2\pi} \frac{I_1(z')}{2\pi a} \frac{\epsilon^{-\gamma R_2}}{R_2} a d\phi_1' dz' \qquad (2\text{-}26)$$

$$R_2 = [2a^2 + 4h^2 + 4ah\cos\phi_0 - 2[a^2 + 4h^2 + 4ah\cos\phi_0]^{\frac{1}{2}} \cdot a\cos(\phi_1 - \phi_1') + (z - z')^2]^{\frac{1}{2}} \qquad (2\text{-}27)$$

$$\phi_1 = \sin^{-1}\left[\frac{a\sin\phi_0}{[a^2 + 4h^2 + 4ah\cos\phi_0]^{\frac{1}{2}}}\right] . \qquad (2\text{-}28)$$

As stated earlier, the currents on the object and image are related by the complex-reflection coefficient for the appropriate angle of incidence and polarization involved. If the cylinders are viewed as consisting of a large number of horizontal dipoles the problem of reflection reduces to that of a horizontal dipole above a finitely conducting ground plane. As pointed out by Jordon [14], in a plane parallel to the axis of the dipole the electric field is parallel to the plane of incidence, vertical polarization. In a plane perpendicular to the axis of the dipole the electric field is perpendicular to the plane of incidence, horizontal polarization. The reflection coefficients for horizontal and vertical polarization, as derived by Jordon [14], are respectively:

$$R_h = \frac{\sin\psi - [(\epsilon_r + x) - \cos^2\psi]^{\frac{1}{2}}}{\sin\psi + [(\epsilon_r + x) - \cos^2\psi]^{\frac{1}{2}}} \qquad (2\text{-}29)$$

$$R_v = \frac{(\epsilon_r + x)\sin\psi - [(\epsilon_r + x) - \cos^2\psi]^{\frac{1}{2}}}{(\epsilon_r + x)\sin\psi + [(\epsilon_r + x) - \cos^2\psi]^{\frac{1}{2}}} \qquad (2\text{-}30)$$

where $x = \frac{\sigma}{s\epsilon_0}$

ϵ_r = relative permittivity of earth

σ = conductivity of earth

ϵ_0 = free space permittivity.

When the plane of incidence is neither in a plane parallel or perpendicular to the axis of the dipole a combination of vertical and horizontal reflection coefficients must be used. The reflection coefficient for this case is given by

$$R_F = R_h \cos\beta - R_v \sin\beta \ldots \qquad (2\text{-}31)$$

The minus sign comes from Jordon's assumed positive directions of electric fields for the incident and reflected waves [14]. Figure 2-5 defines the geometry of the reflection coefficient. Since uniform circumferential current has been assumed no generality will be lost by restricting the field point of the object cylinder to lie along the line $\phi_0 = 0$. With this objective and image current related by

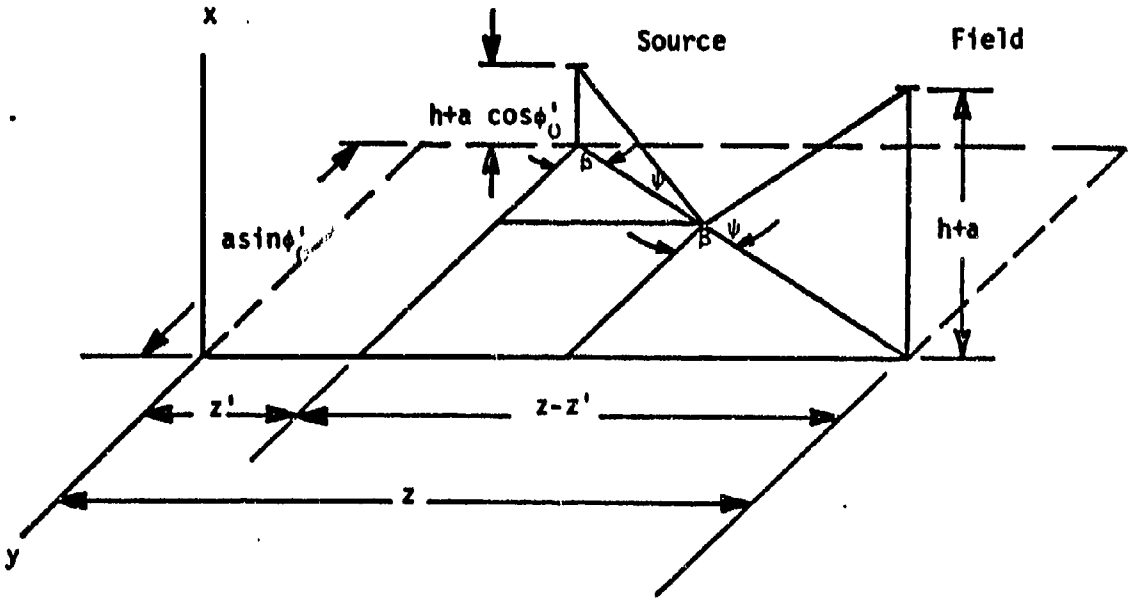

Figure 2-5. Geometry of Reflection Coefficient

$$I_1(z') = R_F I_0(z') \tag{2-32}$$

It will be necessary to express the reflection coefficient in terms of the object coordinate system. With this objective in mind the angle ψ and β defined in Figure 2-5 can be expressed as functions of ϕ_0' and z such that,

$$\psi = \tan^{-1}\left[\frac{2h + a(1 + \cos\phi_0')}{(a^2 \sin^2\phi_0' + (z - z')^2)^{\frac{1}{2}}}\right] \tag{2-33}$$

and

$$\beta = \tan^{-1}\left[\frac{(z - z')}{a \sin\phi_0'}\right] . \tag{2-34}$$

Substituting for ψ and β in equations (2-29), (2-30), and (2-31) yields

$$R_F = \frac{1 - \left[\frac{(\epsilon_r + x - 1)}{\sin^2\psi} + 1\right]^{\frac{1}{2}}}{1 + \left[\frac{(\epsilon_r + x - 1)}{\sin^2\psi} + 1\right]^{\frac{1}{2}}} \frac{a \sin\phi_0'}{(a^2 \sin^2\phi_0' + (z - z')^2)^{\frac{1}{2}}}$$

(2-35)

$$- \frac{(\epsilon_r + x) - \left[\frac{(\epsilon_r + x - 1)}{\sin^2\psi} + 1\right]^{\frac{1}{2}}}{(\epsilon_r + x) + \left[\frac{(\epsilon_r + x - 1)}{\sin^2\psi} + 1\right]^{\frac{1}{2}}} \frac{(z - z')}{(a^2 \sin^2\phi_0' + (z-z')^2)^{\frac{1}{2}}}$$

Dropping the current subscripts of equation (2-32) the magnetic vector potentials become

$$A_{0z}(\phi_0,z) = \frac{\mu_0}{4\pi} \int_0^L \int_0^{2\pi} \frac{I(z')}{2\pi a} \frac{\epsilon^{-\gamma R_1}}{R_1} a d\phi_0' dz' \tag{2-36}$$

$$A_{1z}(\phi_0,z) = \frac{\mu_0}{4\pi} \int_0^L \int_0^{2\pi} \frac{R_F I(z')}{2\pi a} \frac{\epsilon^{-\gamma R_2}}{R_2} a d\phi_1' dz' \tag{2-37}$$

The total field consists of the incident and scattered field, where the scattered field is that due to the current, I(z'). To insure uniqueness the total field must satisfy certain boundary conditions [18].

$$\bar{E}_T = \bar{E}_{inc} + \bar{E}_s. \tag{2-38}$$

The scattered field is related to the induced currents and charges by

$$\bar{E}_s(R) = -s\bar{A}_s(\bar{R}) - \nabla\phi_s(\bar{R}), \tag{2-39}$$

where $\bar{A}_s(\bar{R})$ = the total "scattered" magnetic vector potential

ϕ_s = the total "scattered" electric scalar potential,

which can be related to $\bar{A}_s$ through the Lorentz gauge condition,

$$\phi^s(\bar{R}) = \frac{\nabla \cdot \bar{A}_s(\bar{R})}{-\mu_0 \epsilon_0 s}. \tag{2-40}$$

Equation (2-41) becomes

$$\bar{E}_s(\bar{R}) = -s\left[\bar{A}_s(\bar{R}) - \frac{1}{\mu_0 \epsilon_0 s^2} \nabla[\nabla \cdot \bar{A}_s(\bar{R})]\right]. \tag{2-41}$$

since $\gamma = \frac{s}{c}$ and $c = 1/\sqrt{\mu_0 \epsilon_0}$, $\gamma^2 = s^2 \mu_0 \epsilon_0$. Then,

$$\bar{E}_s(\bar{R}) = -s\left[\bar{A}_s(\bar{R}) - \frac{1}{\gamma^2} \nabla[\nabla \cdot \bar{A}_s(\bar{R})]\right] . \tag{2-42}$$

On the surface of the object cylinder, the boundary condition is

$$\hat{n} \times \bar{E}_T = 0, \tag{2-43}$$

with $\hat{n}$ being the outward normal unit vector on the cylinder surface. An equivalent representation of the boundary condition is

$$E_{inc_{tan}}\Big]_{S_0} = -E_{s_{tan}}\Big]_{S_0} \tag{2-44}$$

which means that the tangential components of the incident and scattered fields must cancel on the object surface for boundary conditions to be satisfied. With the above consideration equation (2-42) becomes

$$E_{inc_{tan}}\Big]_{S_0} = s\left[\bar{A}_s(\bar{R}) - \frac{1}{\gamma^2} \nabla[\nabla \cdot \bar{A}_s(\bar{R})]\right] . \tag{2-45}$$

since

$$\bar{A}_s(\bar{R}_0) = \bar{A}_{0_s} + \bar{A}_{1_s} = A_{0_z}\hat{a}_z + A_{1_z}\hat{a}_z, \tag{2-46}$$

$$\bar{A}_s(\bar{R}_0)\Big]_{S_0} = \hat{a}_z \frac{\mu_0}{4\pi} \int_0^L \int_0^{2\pi} \frac{I(z')}{2\pi a} \frac{e^{-\gamma R_1}}{R_1} a\, d\phi_0' dz'$$

$$+ \int_0^L \int_0^{2\pi} \frac{R_F I(z')}{2\pi a} \frac{e^{-\gamma R_2}}{R_2} a\, d\phi_1' dz' \tag{2-47}$$

Substituting (2-47) into (2-45) one arrives at

$$E_{inc_{tan}}\Big|_{s_0} = s\left[1 - \frac{1}{\gamma^2}\nabla(\nabla\cdot)\right]\hat{a}_z\,\frac{\mu_0}{4\pi}\cdot$$

$$\left\{\int_0^L\int_0^{2\pi}\frac{I(z')}{2\pi a}\,\frac{\varepsilon^{-\gamma R_1}}{R_1}\,a\,d\phi_0'dz' + \int_0^L\int_0^{2\pi}\frac{R_F I(z')}{2\pi a}\,\frac{\varepsilon^{-\gamma R_2}}{R_2}\,a\,d\phi_1'dz'\right\} \tag{2-48}$$

Since

$$(-4\pi\varepsilon_0 s)s\left[1 - \frac{1}{\gamma^2}\nabla(\nabla\cdot)\right]\frac{\mu_0}{4\pi} = -\mu_0\varepsilon_0 s^2\left[1 - \frac{1}{\gamma^2}\nabla(\nabla\cdot)\right]$$

$$= \frac{-s^2}{c^2}\left[1 - \frac{1}{\gamma^2}\nabla(\nabla\cdot)\right] = -\gamma^2\left[1 - \frac{1}{\gamma^2}\nabla(\nabla\cdot)\right]$$

$$= [\nabla(\nabla\cdot) - \gamma^2] \tag{2-49}$$

[2-48] becomes

$$-4\pi\varepsilon_0 s\left(E_{inc_z}\Big|_{s_0}\right) = [\nabla(\nabla\cdot) - \gamma^2]\left\{\int_0^L\int_0^{2\pi}\frac{I(z')}{2\pi a}\,\frac{\varepsilon^{-\gamma R_1}}{R_1}\cdot\right.$$

$$\left.a\,d\phi_0'dz' + \int_0^L\int_0^{2\pi}\frac{R_F I(z')}{2\pi a}\,\frac{\varepsilon^{-\gamma R_2}}{R_2}\,a\,d\phi_1'dz'\right\}. \tag{2-50}$$

The differential operator, $[\nabla(\nabla\cdot) - \gamma^2]$, in the above equation reduces to

$$\left(\frac{\partial^2}{\partial z^2} - \gamma^2\right) \tag{2-51}$$

since equation (2-50) has only a z component. Finally (2-50) reduces to

$$-4\pi\varepsilon_0 s\left(E_{inc_z}\Big|_{s_0}\right) = \left(\frac{\partial^2}{\partial z^2} - \gamma^2\right)\left\{\int_0^L \int_0^{2\pi} \frac{I(z')}{2\pi a}\,\frac{\varepsilon^{-\gamma R_1}}{R_1}\,a\,d\phi'_0 dz'\right.$$

$$\left. + \int_0^L \int_0^{2\pi} \frac{R_F I(z')}{2\pi a}\,\frac{\varepsilon^{-\gamma R_2}}{R_2}\,a\,d\phi'_1 dz'\right\}. \qquad (2\text{-}52)$$

The incident field as shown in Figure 2-2 can be expressed as

$$\bar{E}_{inc} = E_0 \exp[-\gamma(z\cos\theta - x\sin\theta)][\cos\theta\,\hat{a}_x + \sin\theta\,\hat{a}_z]$$
$$- R_v E_1 \exp[-\gamma(z\cos\theta + x\sin\theta)](\cos\theta\,\hat{a}_x - \sin\theta\,\hat{a}_z) \qquad (2\text{-}53)$$

where R_v is as defined in equation (2-30). The minus sign again comes from assumed positive directions of electric fields for the incident and reflected waves in the derivation of R_v [4]. Since only the axial component of the incident field is to be used,

$$E_{z_{inc}} = E_0 \exp[-\gamma(z\cos\theta - x\sin\theta]\sin\theta$$
$$+ R_v E_1 \exp[-\gamma(z\cos\theta + x\sin\theta)]\sin\theta. \qquad (2\text{-}54)$$

The axial component of the transmitted field is

$$E_{z_{tran}} = (1 - R_v)E_0 \exp[-\gamma(z \cos\theta - x \sin\theta)]\sin\theta \qquad (2\text{-}55)$$

To determine E_1 the fields must satisfy the boundary condition

$$E^{tan}_{z_{tran}}\Big|_{x=-h} = E^{tan}_{z_{inc}}\Big|_{x=-h} . \qquad (2\text{-}56)$$

The incident field was defined to contain the direct and reflected field, therefore

$$(1 - R_v)E_0 \exp[-\gamma(z \cos 0 + h \sin\theta)]\sin\theta =$$

$$E_0 \exp[-\gamma(z \cos\theta + h \sin\theta)]\sin\theta +$$

$$R_v E_1 \sin\theta \exp[-\gamma(z \cos\theta - h \sin\theta)] \qquad (2\text{-}57)$$

And upon simplification

$$E_1 = -E_0 \exp[-\gamma\, 2h \sin\theta]. \qquad (2\text{-}58)$$

Substituting (2-58) into (2-54), and evaluating $E_{z_{inc}}$ on the cylinder axis (approximate kernel), instead of on its surface,

$$E_{z_{inc}} = E_0 \exp[-\gamma\, z \cos\theta]\sin\theta \left(1 - R_v \exp[-\gamma\, 2h \sin\theta]\right) . \qquad (2\text{-}59)$$

As stated earlier we have restricted the field point on the object to lie along the line $\phi_0 = 0$. With this restriction

$$R_1 = [2a^2 - 2a^2 \cos(\phi_0 - \phi_0') + (z - z')^2]^{\frac{1}{2}} \qquad (2\text{-}60)$$

and

$$R_2 = [2a^2 + 4h^2 + 4ah\cos\phi_0 - 2(a^2 + 4h^2 + 4ah\cos\phi_0)^{\frac{1}{2}} \cdot a\cos(\phi_1 - \phi_1') + (z - z')^2] \quad (2\text{-}61)$$

where

$$\phi_1 = \sin^{-1}\left[\frac{a\sin\phi_0}{[a^2 + 4h^2 + 4ah\cos\phi_0]^{\frac{1}{2}}}\right] . \quad (2\text{-}62)$$

Reduces to

$$r_1 = R_1\Big|_{\phi_0=0^\circ} = [2a^2(1 - \cos\phi_0') + (z - z')^2]^{\frac{1}{2}} \quad (2\text{-}63)$$

$$r_2 = R_2\Big|_{\phi_0=0^\circ} = [(2a^2 + 4ah)(1 - \cos\phi_1') + 4h^2 + (z - z')^2]^{\frac{1}{2}}. \quad (2\text{-}64)$$

Let

$$1 - \cos\phi_0' = 2\sin^2\frac{\phi_0'}{2} \quad (2\text{-}65)$$

and d = diameter of the cylinder

$$= 2a \quad (2\text{-}66)$$

so

$$r_1 = \left[a^2\sin^2\frac{\phi_0'}{2} + (z - z')^2\right]^{\frac{1}{2}} \quad (2\text{-}67)$$

$$r_2 = [(d^2 + 8ah)\sin^2\frac{\phi_1'}{2} + 4h^2 + (z - z')^2]^{\frac{1}{2}} \quad (2\text{-}68)$$

Also defining two functions

$$f_0(z,z',s) = \int_0^{2\pi} \frac{\epsilon^{-\gamma r_1}}{r_1} a d\phi_0' \tag{2-69}$$

and

$$f_1(z,z',s) = \int_0^{2\pi} \frac{\epsilon^{-\gamma r_2}}{r_2} a d\phi_1' \tag{2-70}$$

Equation (2-52) becomes

$$-4\pi\epsilon_0 s[E_{inc_z}]\Big|_{s_0} = \left(\frac{\partial^2}{\partial z^2} - \gamma^2\right) \left\{\int_0^L \frac{I(z')}{2\pi a} (f_0 + R_F f_1) dz'\right\} \tag{2-71}$$

Where $E_{z_{inc}}$ is given by equation (2-59). In order to better represent the complex frequency dependence,

$$(-4\pi\epsilon_0 s)\left(E_0 \sin\theta\, \epsilon^{-\gamma z \cos\theta}[1 - R_v \epsilon^{-\gamma 2h \sin\theta}]\right) =$$

$$\int_0^L \frac{I(z',s)}{2\pi a} \left(\frac{\partial^2}{\partial z^2} - \gamma^2\right) [f_0(z,z',s) + R_F f_1(z,z',s)] dz'. \tag{2-72}$$

This is the integro-differential equation to be solved for the unknown induced current.

Application of the Moment Method

The integro-differential equation shall be cast into matrix form suitable for a numerical solution; this process is called the method of mements [19], [20], [21 - 22]. The portion of the cylinder at ϕ_0=0, "a thin wire", is broken into N small zones, with the induced current on each of these zones assumed to be constant. The integration over the "wire" is now approximated by the sum of integrals over N segments.

Current on the wire may be described by the function

$$I(z',s) = \sum_n \alpha_n(s) I_n(z') \tag{2-73}$$

where

α_n = unknown coefficient of constant current on n^{th} subsection

and

$$I_n(z') = \begin{cases} 1, \text{ for } z^n < z < z^{n+1} \\ 0, \text{ elsewhere} \end{cases} \tag{2-74}$$

In Figure 2-6 is shown the geometry pertaining to the method of moments. The boundary condition that current at wire ends be zero is automatically satisfied by allowing the two end zones to extend past the surface of the cylinder. Zone length, match points, and end points are given respectively by

$$\Delta = L/(N-1) = \text{length of a zone} \tag{2-75}$$

$$z_m = (m-1)\Delta, \; m = 1,2,\ldots,N \tag{2-76}$$

$$z^n = (n-3/2)\Delta, \; n = 1,2,\ldots,N+1 \tag{2-77}$$

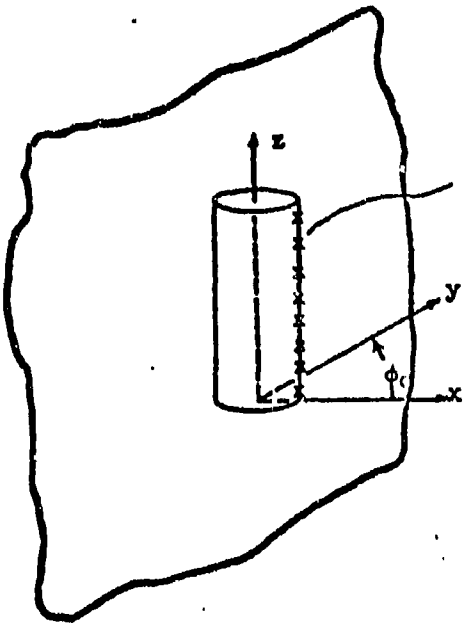

MATCH POINTS ON CYLINDER SURFACE AT $\phi_o = 0°$

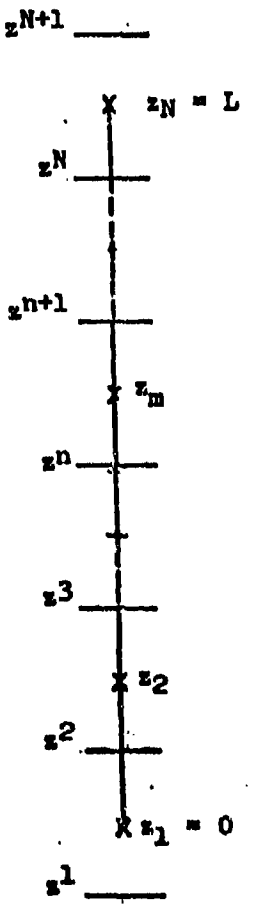

"WIRE"

SUBSECTION ENDS

X MATCH POINTS

$z_m = (m-1)\Delta$ (MATCH POINTS)
$m = 1,2,...N$

$z^n = (n-3/2)\Delta$ (SUBSECTION ENDS)
$n = 1,2,...N+1$

$\Delta = L/(N-1)$ LENGTH OF ZONE

N = NUMBER OF SUBSECTIONS

Figure 2-6. Moment Method Partitioning of Geometry

where L = length of wire

N = number of zones.

With current on the wire expressed as a pulse function, the integro-differential equation (2-72) may be written as

$$(-4\pi\epsilon_0 s)\left\{E_0 \sin\theta\, e^{-\gamma z\cos\theta}[1-R_v e^{-\gamma 2h\sin\theta}]\right\} =$$

$$\sum_n \alpha_n(s) \int_{z^n}^{z^{n+1}} \frac{1}{2\pi a}\left(\frac{\partial^2}{\partial z^2} - \gamma^2\right)[F_0(z,z',s)-R_F F_1(z,z',s)]dz'. \tag{2-78}$$

This equation is to be satisfied at discrete match points, these points being described by equation (2-76). Derivatives in equation (2-78) will be approximated by a finite difference technique, that is

$$\frac{d^2F}{dz^2} = \frac{1}{(\Delta z)^2}[F(z+\Delta z) - 2F(z) + F(z-\Delta z)]. \tag{2-79}$$

Using (2-79) in (2-78) yields

$$(-4\pi\epsilon_0 s)\left\{E_0 \sin\theta\, e^{-\gamma z_m\cos\theta}\,[1 - R_v\, e^{-\gamma 2h\sin\theta}]\right\} =$$

$$\sum_n \frac{\alpha_n(s)}{2\pi a}\,\frac{1}{\Delta^2}\int_{z^n}^{z^{n+1}} \Big\{F_0(z_{m+1},z',s)-(\gamma^2\Delta^2+2)F_0(z_m,z',s)$$

$$+ F_0(z_{m-1},z',s) - R_F[F_1(z_{m+1},z',s)-(\gamma^2\Delta^2+2)F_1(z_m,z',s)$$

$$+ F_1(z_{m-1},z',s)]\Big\}\,dz' \qquad \begin{matrix} n = 2,3,\ldots,N-1 \\ m = 2,3,\ldots,N-1 \end{matrix} \tag{2-80}$$

where $$R_F = \frac{1 - \left[\frac{(A-1)}{B} + 1\right]^{\frac{1}{2}}}{1 + \left[\frac{(A-1)}{B} + 1\right]^{\frac{1}{2}}} \frac{a \sin \phi_0'}{[a^2 \sin^2 \phi_0' + (z_m - z')]^{\frac{1}{2}}}$$

$$- \frac{A - \left[\frac{(A-1)}{B} + 1\right]^{\frac{1}{2}}}{A + \left[\frac{(A-1)}{B} + 1\right]^{\frac{1}{2}}} \frac{(z_m - z')}{[a^2 \sin^2 \phi_0' + (z_m - z')]^{\frac{1}{2}}} \qquad (2\text{-}81)$$

$$A = \epsilon_r + \frac{\sigma}{s\epsilon_0} \qquad (2\text{-}82)$$

$$B = \sin^2 \psi, \psi = \tan^{-1} \left\{ \frac{2h + a(1 + \cos \phi_0')}{[a^2 \sin^2 \phi_0' + (z_m - z')^2]^{\frac{1}{2}}} \right\} . \qquad (2\text{-}83)$$

This equation may be manipulated into the form

$$\bar{V}(s) = \bar{\bar{Z}}(s)\bar{I}(s) \qquad (2\text{-}84)$$

where a single bar represents a column matrix or vector and a double bar indicates a square matrix.

Let $\bar{V}(s)$ = the source vector = $[v_m]$

where v_m = the matrix elements of $\bar{V}(s)$

$$= (-4\pi\epsilon_0 s) \left\{ E_0 \sin \theta \, e^{-\gamma z_m} [1 - R_v e^{-\gamma 2h \sin \theta}] \right\}$$

$$m = 2,3,\ldots,N-1; \qquad (2\text{-}85)$$

$\bar{\bar{Z}}(s)$ = the impedance matrix = $[z_{mn}]$,

where z_{mn} = the matrix elements of $\bar{\bar{Z}}(s)$

$$= \frac{1}{\Delta^2} \int_{z_n}^{z^{n+1}} \frac{1}{2\pi a} \Big\{ [F_0(z_{m+1},z',s) - (\gamma^2\Delta^2+2)F_0(z_m,z',s) + F_0(z_{m-1},z',s)] - R_F[F_1(z_{m+1},z',s) - (\gamma^2\Delta^2+2) F_1(z_m,z',s) + F_1(z_{m-1},z',s)] \Big\} dz'$$

$$n = 2,3,\ldots,N-1$$

$$m = 2,3,\ldots,N-1 \qquad (2\text{-}86)$$

and $\bar{I}(s)$ = the response vector = $[i_n]$,

where i_n = the matrix elements of $\bar{I}(s)$

= α_n, unknown coefficient of constant current in the n^{th} zone $\qquad n = 2,3,\ldots,N-1 \qquad (2\text{-}87)$

The unwieldy appearance of equation (2-86) may be somewhat improved by defining two functions

$$H_{0_{mn}}(z_m,s) = \int_{z_n}^{z^{n+1}} \int_0^{2\pi} \frac{e^{-\gamma r_1}}{r_1} d\phi_0' dz' \qquad (2\text{-}88)$$

with $$r_1 = [d^2 \sin^2 \frac{\phi_0'}{2} + (z_m - z')^2]^{\frac{1}{2}} \qquad (2\text{-}89)$$

and $$H_{1_{m\,n}}(z_m,s) = \int_{z^n}^{z^{n+1}} \int_0^{2\pi} \frac{e^{-\gamma r_2}}{r_2} d\phi_1' dz' \qquad (2\text{-}90)$$

with $$r_2 = [(d^2 + 8ah)\sin^2 \frac{\phi_1'}{2} + 4h^2 + (z_m - z')^2]^{\frac{1}{2}}. \qquad (2\text{-}91)$$

Now equation (2-86) may be redefined as

$$z_{m\,n} = \frac{1}{2\pi\Delta^2} \left\{ H_{0_{m\,n}}(z_{m+1},s) - (\gamma^2\Delta^2+2)H_{0_{m\,n}}(z_m,s) \right.$$

$$+ H_{0_{m\,n}}(z_{m-1},s) - R_F[H_{1_{m\,n}}(z_{m+1},s) - (\gamma^2\Delta^2+2)H_{1_{m\,n}}(z_m,s)$$

$$\left. + H_{1_{m\,n}}(z_{m-1},s)] \right\}. \qquad (2\text{-}92)$$

When $\phi_0' = 0°$ and $z' = z_m$ then $r_1 = 0$, (see equation (2-89)) thus the integrand of $H_{0_{m\,n}}(z_m,s)$, see equation (2-88), will be singular. Tesche [23] provides methods of evaluating integrals of this type. Note that the integrand of $H_{1_{m\,n}}(z_m,s)$ is never singular due to the term $4h^2$ in equation (2-91).

At $\phi_0' = 0°$, the integrand of $H_{0_{m\,n}}(z_{m+1},s)$ is singular when $z_{m+1} = z'$, where $z^n \leq z' \leq z^{n+1}$. Hence, at this point,

$$z^n \leq z_{m+1} \leq z^{n+1}. \qquad (2\text{-}93)$$

Using equation (2-76) and (2-77) it is seen that the singularity occurs when

$$-3/2 \leq (m-n) \leq -1/2. \qquad (2\text{-}94)$$

m and n are integers, therefore $H_{0_{m\,n}}(z_m,s)$ is singular when $m-n = -1$ or when $m=n-1$. A similar argument may be applied to show that $H_{0_{m\,n}}(z_m,s)$ is singular when $m=n$ and that $H_{0_{m\,n}}(z_{m-1},s)$ is singular when $m=n+1$.

Following the procedure outlined by Tesche [23], let the integral of $H_{0_{m\,n}}(z_m,s)$ at its singularity be T_1.

$$T_1 = H_{0_{m\,n}}(z_m,s) \qquad \text{when } m=n, \tag{2-95}$$

where $H_{0_{m\,n}}(z_m,s)$ is given by equation (2-88). Transform variables in (2-88) as follows:

$$\begin{aligned} \text{let} \qquad \phi &= \phi_0' \\ z &= z_m - z' \\ dz &= -dz' \end{aligned} \tag{2-96}$$

and the limits of integration become

$$\begin{aligned} z^n \Big\rfloor_{m=n} &= z_m - z^n \Big\rfloor_{m=n} = \Delta/2 \\ z^{n+1} \Big\rfloor_{m=n} &= z_m - z^{n+1} \Big\rfloor_{m=n} = -\Delta/2 \end{aligned} \tag{2-97}$$

Thus,

$$T_1 = \int_{-\frac{\Delta}{2}}^{\frac{\Delta}{2}} \int_0^{2\pi} \frac{e^{-\gamma r_1}}{r_1}\, d\phi dz \tag{2-98}$$

where $r_1 = [z^2 + d^2 \sin^2 \phi/2]^{\frac{1}{2}}$

Define $T_2 = H_{0_{m\,n}}(z_{m+1},s)$ when $m = n-1$ (2-99)

and $T_3 = H_{0_{m\,n}}(z_{m-1},s)$ when $m = n+1$ (2-100)

it can be shown that $T_1 = T_2 = T_3$.

Equation (2-98) may be prepared for numerical evaluation by following a procedure similar to that used by Tesche [23]. A Maclaurin series for $e^{-\gamma r_1}$ is as follows:

$$e^{-\gamma r_1} = 1 - \gamma r_1 + \frac{r_1^2\gamma^2}{2!} - \frac{r_1^3\gamma^3}{3!} + \ldots \frac{(-1)^n r^n \gamma^n}{n!} + \ldots$$

$$= \sum_{n=0}^{\infty} \frac{(-r_1\gamma)^n}{n!} \qquad (2\text{-}101)$$

Using only the first two terms of (2-101) equation (2-98) may be written as

$$T_1 = \left(\int_0^{2\pi} \int_{-\Delta/2}^{\Delta/2} \frac{1}{r_1} \, d\phi dz \right) - 2\pi\Delta\gamma \qquad (2\text{-}102)$$

also
$$\int_{-\Delta/2}^{\Delta/2} \frac{dz}{r_1} = 2\ell n \left\{ \frac{\Delta}{2d} + \left[\left(\frac{\Delta}{2d} \right)^2 + \sin^2 \frac{\phi}{2} \right]^{\frac{1}{2}} \right\} - 2\ell n(\sin \tfrac{\phi}{2}) \qquad (2\text{-}103)$$

and therefore

$$T_1 = 2 \int_0^{2\pi} \ell n \left\{ \frac{\Delta}{2d} + \left[\left(\frac{\Delta}{2d} \right)^2 + \sin^2 \frac{\phi}{2} \right]^{\frac{1}{2}} \right\} d\phi$$

$$- 2 \left(\int_0^{2\pi} \ell n(\sin \tfrac{\phi}{2}) d\phi \right) - 2\pi\Delta\gamma. \qquad (2\text{-}104)$$

The first term in the above equation is non-singular and can be evaluated numerically, the second term is easily evaluated analytically be expressing $\ell n(\sin \phi/2)$ in a series, that is,

$$\ell n(\sin \phi/2) = -\ell n\ 2 - \sum_{n=1}^{\infty} \frac{1}{n} \cos n\phi \qquad (2\text{-}105)$$

so
$$\int_0^{2\pi} \ell n(\sin \phi/2) = -2\pi\ \ell n\ 2 - \sum_{n=1}^{\infty} \frac{1}{n} \int_0^{2\pi} \cos n\phi d\phi \qquad (2\text{-}106)$$

Finally,

$$T_1 = 2 \left\{ \int_0^{2\pi} \ell n \left[\frac{\Delta}{2d} + \left\{ \left(\frac{\Delta}{2d} \right)^2 + \sin^2 \phi/2 \right\}^{\frac{1}{2}} \right] d\phi \right.$$

$$\left. + \pi(\ell n\ 4 - \Delta\gamma) \right\} . \qquad (2\text{-}107)$$

The integro-differential equation has been cast as a system of matrices, which may be solved for the unknown induced current.

Application of the Singularity Expansion Method

The singularity expansion method (SEM), formalized by Baum [23-25], and applied by many others [1-3], [26], [27-30], is a method for characterizing the response of scattering objects illuminated by either transient or steady-state electromagnetic radiation. A general outline describing the theory of SEM will be presented with special attention given to areas of interest.

The time domain current may be determined from a knowledge of the exterior natural resonant frequencies of the scatterer in much the same manner as in classical circuit theory. The natural frequencies of the "wire," s_α, are those such that the homogeneous version of equation (2-84)

$$\bar{\bar{Z}}(s)\bar{I}(s) = 0 \tag{2-108}$$

has a non-trivial solution for $I(s_\alpha)$. This implies that the determinant of $\bar{\bar{Z}}$ must vanish at these complex natural frequencies; and therefore the equation for determining these resonances becomes

$$\det \bar{\bar{Z}}(s_\alpha) = 0 \tag{2-109}$$

The natural frequencies must lie in the left-hand portion of the s-plane since exponentially increasing currents are not allowed. Further, the poles must occur in conjugate pairs since the time domain current is real. No poles may reside on the $j\omega$ axis since the radiation process requires that the current on the wire be eventually zero. It is assumed, without proof, that the poles are all simple. This has been substantiated numerically [30].

The matrix equation,

$$\bar{\bar{Z}}(s)\bar{I}(s) = \bar{V}(s) \tag{2-110}$$

has as a solution

$$\bar{I}(s) = \bar{\bar{Z}}^{-1}(s)\bar{V}(s). \tag{2-111}$$

The time domain response is given by the inverse laplace transform in the form

$$i(t) = \frac{1}{2\pi j} \int_{\sigma_0 - j\infty}^{\sigma_0 + j\infty} \bar{\bar{Z}}^{-1}(s)\bar{V}(s)e^{st}ds. \qquad (2\text{-}112)$$

Instead of numerically evaluating this integral along the σ_0 contour, SEM assumes that the inverse of the impedance matrix may be expressed as

$$\bar{\bar{Z}}^{-1}(s) = \sum_{\alpha} \frac{\bar{\bar{R}}_{\alpha}}{s - s_{\alpha}} . \qquad (2\text{-}113)$$

This assumption allows evaluation of equation (2-112) by the Cauchy Residue Theorem. Equation (2-113) is a summation over all poles in the complex s-plane. $\bar{\bar{R}}_{\alpha}$ is defined as the system residue matrix at the pole s_{α}. This residue matrix is a dyadic and can be represented as the outer product of vectors independent of s as

$$\bar{\bar{R}}_{\alpha} = \bar{M}_{\alpha}\bar{C}_{\alpha}^{T} \qquad (2\text{-}114)$$

where $\bar{M}_{\alpha}$ is the natural mode vector and is a solution to

$$\bar{\bar{Z}}(s_{\alpha})\bar{M}_{\alpha} = 0 \qquad (2\text{-}115)$$

and $\bar{C}_{\alpha}$ is the coupling vector, which satisfies the equation

$$\bar{\bar{Z}}(s_{\alpha})^{T}\bar{C}_{\alpha} = 0 \qquad (2\text{-}116)$$

(T denotes transpose). For the electric field formulation, where the impedance matrix is symmetric, i.e. $(\overline{\overline{Z}}(s_\alpha) = \overline{\overline{Z}}^T(s_\alpha))$, the natural mode vector and coupling vector are equal, and therefore

$$\overline{\overline{R}}_\alpha = \overline{C}_\alpha \overline{C}_\alpha^T. \tag{2-117}$$

Let $\overline{C}_\alpha$ be normalized such that its maximum element is real and equal to unity.

$$\overline{C}_\alpha = \sqrt{\beta_\alpha} \quad [C_{\alpha_{\text{normalized}}}] \tag{2-118}$$

and define

$$\overline{C}_{\alpha_{\text{normalized}}} = \overline{C}_{\alpha_0}, \tag{2-119}$$

such that

$$\overline{\overline{R}}_\alpha = \beta_\alpha \overline{C}_{\alpha_0} \overline{C}_{\alpha_0}^T, \tag{2-120}$$

where β_α is the normalization coefficient. Since

$$\overline{\overline{Z}}^{-1}(s) = \sum_\alpha \frac{\beta_\alpha \overline{C}_{\alpha_0} \overline{C}_{\alpha_0}^T}{s-s_\alpha} \tag{2-121}$$

The normalization coefficient is determined through consideration of a particular singularity [2], s_p, such that

$$\overline{C}_p^T \overline{\overline{Z}}(s) \overline{\overline{Z}}^{-1}(s) \overline{C}_p = \overline{C}_p^T \overline{\overline{U}}\, \overline{C}_p = \overline{C}_p^T \overline{C}_p \tag{2-122}$$

(NOTE: $\overline{\overline{U}}$ is the identity matrix.)

Substituting equation (2-121) into (2-122) yields

$$\bar{C}_p^T \bar{\bar{Z}}(s) \sum_\alpha \frac{\beta_\alpha \bar{C}_\alpha \bar{C}_\alpha^T}{s-s_\alpha} \bar{C}_p = \bar{C}_p^T \bar{C}_p$$

or

$$\sum_\alpha \beta_\alpha \frac{\bar{C}_p^T \bar{\bar{Z}}(s) \bar{C}_\alpha \bar{C}_\alpha^T \bar{C}_p}{s-s_\alpha} = \bar{C}_p^T \bar{C}_p. \qquad (2\text{-}123)$$

Note that

$$\bar{C}_p^T \bar{\bar{Z}}(s_p) \bar{C}_\alpha = \bar{C}_p^T \bar{\bar{Z}}(s_p)^{TT} \bar{C}_\alpha \left(\bar{\bar{Z}}(s_p)^T \bar{C}_p\right)^T C_\alpha = 0 \qquad (2\text{-}124)$$

so (2-123) may now be written as

$$\sum_\alpha \beta_\alpha \frac{\bar{C}_p^T [\bar{\bar{Z}}(s) - \bar{\bar{Z}}(s_p)] \bar{C}_\alpha \bar{C}_\alpha^T \bar{C}_p}{s-s_\alpha} = \bar{C}_p^T \bar{C}_p. \qquad (2\text{-}125)$$

By definition,

$$\lim_{s \to s_p} \frac{\bar{\bar{Z}}(s) - \bar{\bar{Z}}(s_p)}{s-s_\alpha} = \bar{Z}'(s_p) \delta_{p\alpha}, \qquad (2\text{-}126)$$

where $\bar{Z}'(s_p) = \left.\frac{d\bar{Z}}{ds}\right|_{s=s_p}$

And $\delta_{p\alpha}$ is the Kronecker delta function. Taking the limit as s approaches s_p in (2-125) results in

$$\beta_p \bar{C}_p^T \bar{Z}'(s_p) \bar{C}_p \bar{C}_p^T \bar{C}_p = \bar{C}_p^T \bar{C}_p, \qquad (2\text{-}127)$$

From which we conclude that

$$\beta_p = \frac{1}{\overline{C}_p^T \overline{Z}'(s_p)\overline{C}_p} . \tag{2-128}$$

Finally,

$$i(t) = \frac{1}{2\pi j} \int_{\sigma_0 - j\infty}^{\sigma_0 + j\infty} \sum_{\alpha} N_\alpha C_{\alpha_0} \frac{e^{st}}{s - s_\alpha} \, ds \tag{2-129}$$

where $N_\alpha = \beta_\alpha \overline{C}_{\alpha_0}^T \overline{V}_\alpha$

is defined as the coupling coefficient. With the matrix elements of $\overline{V}(s)$ defined by (2-85), let the incident field be a step-function plane wave, such that

$$E_0(s) = E_0/s$$

The matrix elements of $\overline{V}(s)$ are then defined as

$$v_m = -4\pi c_0 \left\{ E_0 \sin\theta \, e^{-\gamma z_m} [1 - R_v e^{-\gamma 2h \sin\theta}] \right\} \tag{2-130}$$

where $m = 2,3,\ldots, N-1;$

Evaluating (2-129) through the residue theorem will produce appropriate Heaviside functions, which are viewed as enforcing causality [30], [1-3].

The exponential dependence of (2-129) is expressed by

$$V_m e^{st} = De^{-\gamma z_m}[1 - R_v e^{-\gamma 2h \sin\theta}]e^{st} \tag{2-131}$$

where

$$D = -4\pi\epsilon_0 E_0 \sin\theta.$$

Equation (2-131) can be written as

$$v_m e^{st} = D\left\{e^{s[t - z_m/c]} - R_v e^{s\left[t - \frac{z_m + 2h\sin\theta}{c}\right]}\right\} \tag{2-132}$$

And now (2-129) becomes

$$i(t) = \frac{1}{2\pi j}\int_{\sigma_0 - j\infty}^{\sigma_0 + j\infty} \sum_{\alpha} \frac{\beta_\alpha \bar{C}_{\alpha_0} \bar{C}_{\alpha_0}^{T}}{s - s_\alpha}\, \bar{V}_\alpha(s)\,ds \tag{2-133}$$

$\bar{V}_\alpha(s)$ is a vector with matrix elements defined by (2-132). Stated more simply,

$$\bar{V}_\alpha(s) = [v_m e^{st}] = \bar{V}(s)e^{st}. \tag{2-134}$$

If we let

$$\tau_1 = z_m/c \tag{2-135}$$

and

$$\tau_2 = \frac{z_m + 2h\sin\theta}{c} \tag{2-136}$$

Then the matrix elements of $\bar{V}_\alpha(s)$ are

$$v_m e^{st} = D[e^{s(t-\tau_1)} - R_v e^{s(t-\tau_2)}]. \tag{2-137}$$

Evaluation of (2-133) may be carried out by using the residue theorem.

Note that the complex natural frequencies, natural mode vectors, and normalization coefficients are not functions of the incident field. Only $\overline{V}_\alpha(t)$ is altered upon a change in the angles of incidence. Consequently, once s_α, β_α, and $\overline{C}_{\alpha_0}$ are found for a particular L, h, and a, the current excited by any incident field is easily found.

The singularity expansion method, applied to this transient electromagnetic problem, produces a system of matrices, which are solved for the induced current on the object cylinder as a function of time.

Approximations and Limitations

A summary of the approximations used thus far will be presented so that the results obtained may be viewed in the proper perspective.

The assumptions and approximations are:

1. Current is assumed to flow only in the direction of the cylinder axis.
2. Boundary conditions are enforced only on the axial component of the tangential electric field.
3. End caps on the cylinder are ignored.
4. Current is assumed to be uniformly circumferentially distributed.
5. The moment method is an approximate numerical solution.
6. The "T" function, equation (2-107), for evaluating the singular integral is an approximate solution.
7. The reflection method does not account for the currents induced in the earth.

Assumptions one and two require that the cylinder be thin, $L \gg a$. The third assumption is valid if $a \ll \lambda$, this is seen to be, because

current induced on the end caps will not significantly contribute to the scattered field [31]. Uniform circumferential variation of the current is a valid approximation when the cylinder is many radii away from the ground plane. The assumptions involved in Tesche's solution for the T function places two restrictions on the problem [23]. The main restriction requiring $L >> a$, and secondly this formulation is not applicable to high frequency analysis.

The reflection method, although valid when the cylinder is located far from the ground plane, is not valid when the cylinder is close to the ground plane. Additional terms must be added to the equations to account for the "surface wave" [14]. The term surface wave as used here is as defined by Norton [32]. In a dissertation by Jerry McCannon [16], a study was done of a vertical dipole using several different formulations. The reflection method was found to give answers within 1 to 2 percent of the exact solution when the height of the dipole was greater than $3/8\ \lambda$.

In a recent investigation by Sarkar and Strait [10], it was found that the reflection method for the horizontal electric dipole produced results within 10% of the exact Sommerfeld formulation if

$$h > \frac{.25}{\sqrt{\epsilon_r}}\ \lambda, \qquad (2\text{-}138)$$

where

h = height of the dipole above the ground plane

ϵ_r = relative permittivity of ground plane

λ = free space wave length.

Throughout this study an average of 15 was used for ϵ_r, relative permittivity of earth in this case, which results in $h > .065\ \lambda$.

III. NUMERICAL RESULTS

A computer code has been written to implement the equations developed in the previous section. This code is used to determine the natural resonances and natural mode vectors of the scatterer. The scatterer is described by a general length, radius, and height above the ground plane. The finitely conducting ground plane, assumed nonmagnetic $\mu = \mu_0$, is characterized by σ, the conductivity, and $\epsilon = \epsilon_0\epsilon_r$ the permittivity. Singularities, i.e.(natural resonances), occur in layers in the complex plane and will be described by $s_{\ell,n}$ where "ℓ" denotes the layer of the pole and "n" the pole within the layer, this method of description is that used by Tesche [30]. This data will present trajectories of the first three poles of the first layer, s_{11}, s_{12}, and s_{13}.

Figure 3-1 shows the movement of the singularity s_{11} in the complex plane as several system parameters are varied. The outer dashed spiral through the points labeled A describes the movement of the pole s_{11} as the scatterer is brought near the ground plane, the conductivity is held constant at $\sigma = 120.0$ along this curve. It may be concluded that the Q of the scatterer stabilizes as h/ℓ becomes large since the dashed spiral seems to become confined to a smaller area in the s-plane. For each value of h/ℓ, the conductivity is varied from $\sigma = 120$, point A on the dashed curve, to $\sigma = 1.2 \times 10^{-4}$, point G; intermediate values are shown at points B through F. The value $\sigma = 1.2 \times 10^{-3}$ and $\sigma = 1.2 \times 10^{-2}$ at points E and F respectively correspond to typical values of conductivity

for normal terrain. Let the paths traversed by the pole for a given value h/ℓ be called the inner spirals. It is seen that each inner spiral, corresponding to a given value of h/ℓ, converges to point G as the conductivity of the ground plane is reduced, this result is to be expected since point G is the location of s_{11} for free space conditions [29]. When the pole is displaced from position G along one of the inner spirals more energy is being reflected from the ground plane, this follows from the fact the incident illumination experiences a greater discontinuity as the value of σ is increased. In the limit as σ becomes very large all the incident energy would be reflected and the problem becomes that of a cylindrical scatter over a perfectly conducting ground plane. Figure 3-2 is also a plot of s_{11} as the value of h/ℓ and σ vary, the relative permittivity is held at five. Unlike Figure 3-1, point G is not the same in the limiting case of small σ, but rather each inner spiral converges to some point along an inner dashed spiral. Although the conductivity becomes small the relative permittivity remains at five, thus the incident wave will meet some discontinuity and there will be energy reflected from the ground plane. Figures 3-3 and 3-4 display similar information as described above. In Figure 3-3 and 3-4 the relative permittivity is fifteen and one hundred respectively, as σ again gets small point B is further from that of the free space position due to the larger values of ϵ_r. To summarize, displacement of the singularity from its free space position is a function of the magnitude of discontinuity in the ground plane whether it be produced by the conductivity or relative permittivity. Figures 3-5 through 3-8

may be interpreted similarly. Note that in Figures 3-5 and 3-7 the inner spirals cross the outer dashed spiral, this is most probably due to numerical error. When the method of moments is employed, a rule of thumb is to choose the number of zones, N, in accordance with $N = 10 \times sL/\pi c$. This implies that if $s = j\omega$, ten cells per half-wavelength are used [30]. This rule was adhered to for pole s_{11}, the first resonance of the scatterer, but N was not changed for s_{12}, or s_{13} this means that there were only 5 zones per half wavelength for s_{12}, and 3 zones per half wavelength for s_{13}.

The real and imaginary part of the normalized mode vector for the singularities s_{11}, and s_{12}, are shown in Figures 3-9 through 3-12. Note that the modes are either even or odd functions about the scatterer midpoint. It is also seen that the imaginary part of the mode vector is much less than the real part, indicating the modes are almost real functions of position. The conductivity and relative permittivity were also varied when calculating the normal mode vectors, results showed the normal mode vectors being relatively independent of these quantities.

Figure 3-1. Trajectory of Singularity S_{11} $\epsilon_R=1$

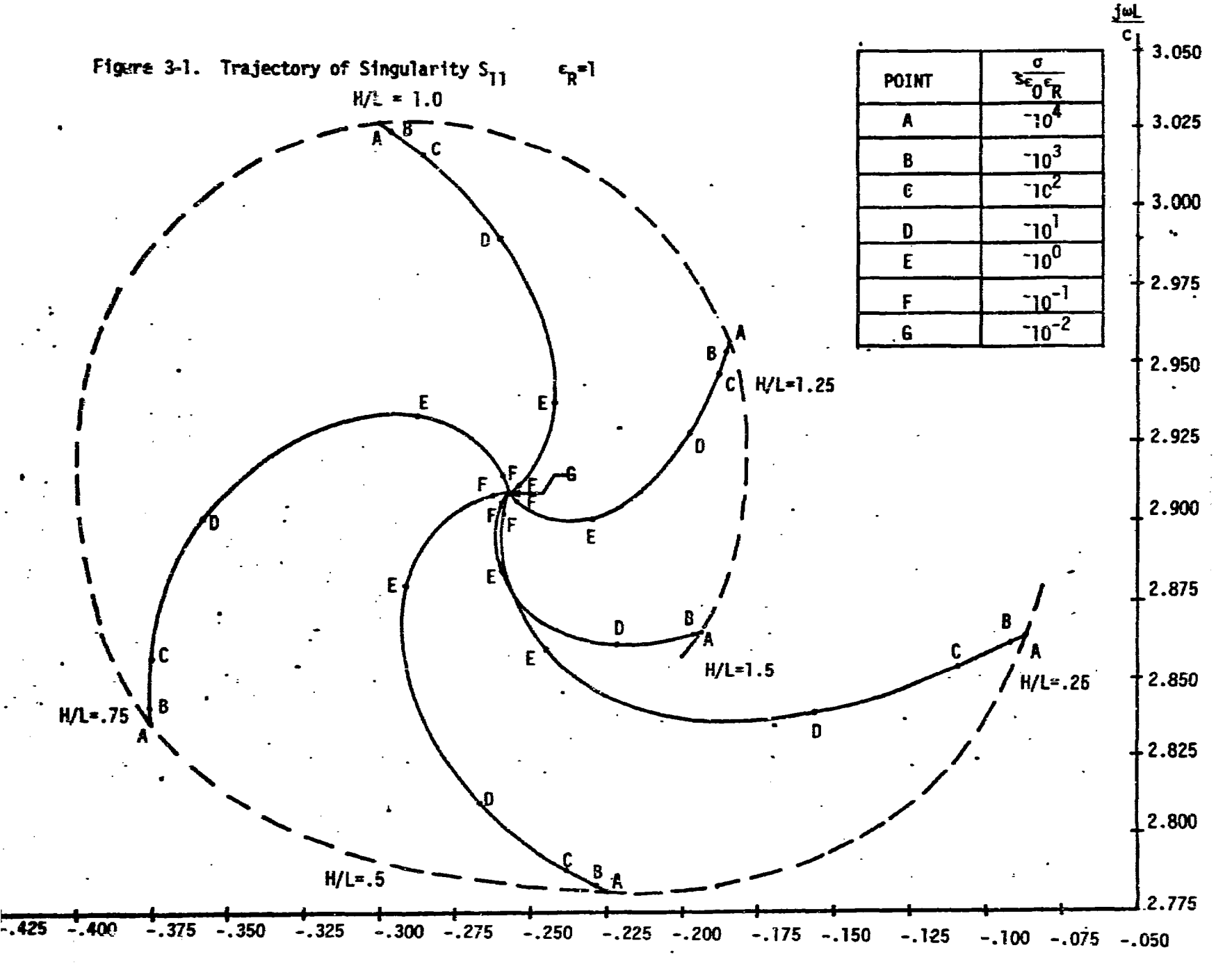

POINT	$\frac{\sigma}{3\epsilon_0\epsilon_R}$
A	-10^4
B	-10^3
C	-10^2
D	-10^1
E	-10^0
F	-10^{-1}
G	-10^{-2}

FIG 3 - 2

Trajectory of Singularity S_{11}

$\varepsilon_R = 5$

POINT	$\frac{\sigma}{s\varepsilon_0\varepsilon_R}$
A	-10^3
B	-10^2
C	-10^1
D	-10^0
E	-10^{-1}
F	-10^{-2}
G	-10^{-3}

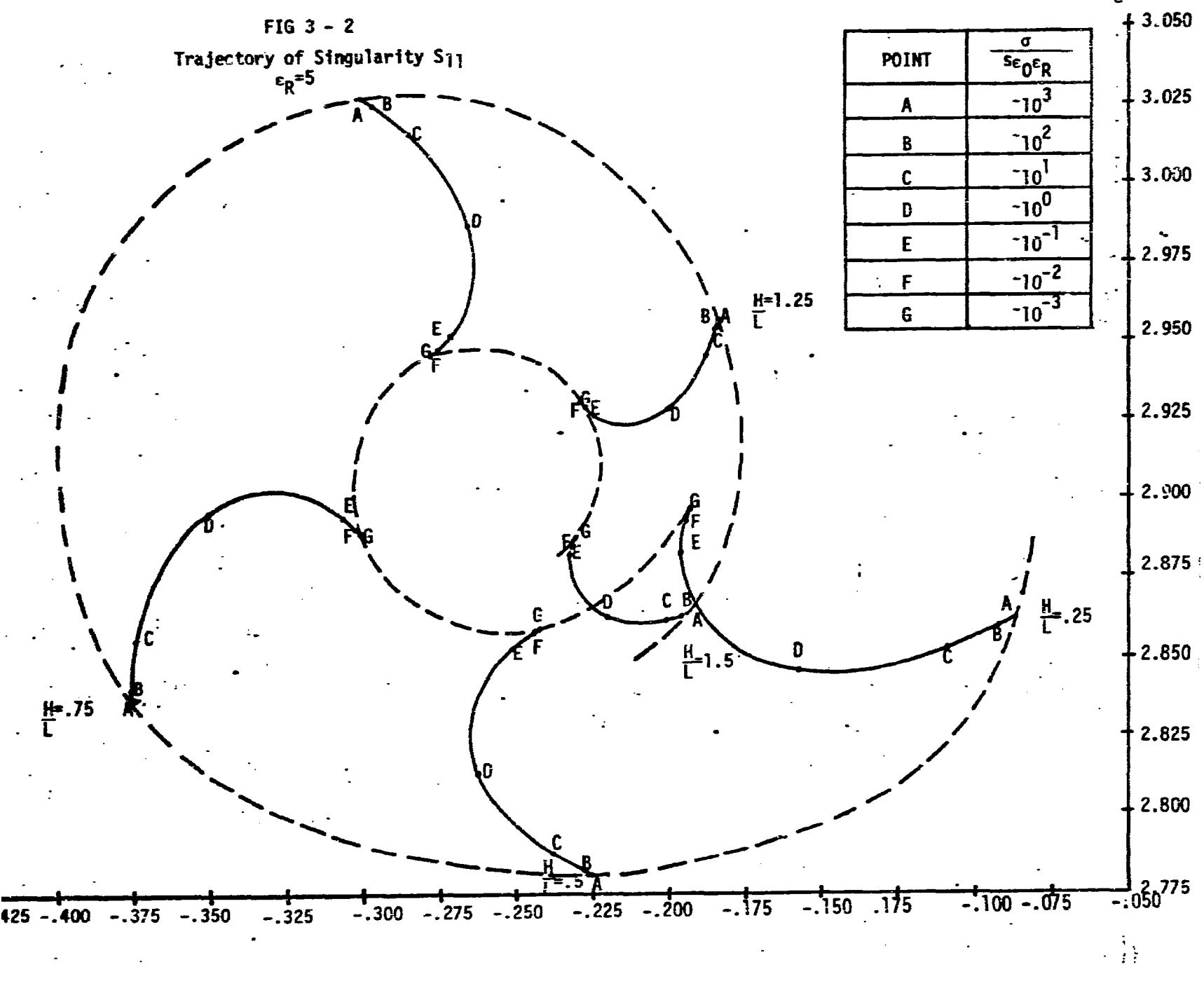

FIG 3 - 3

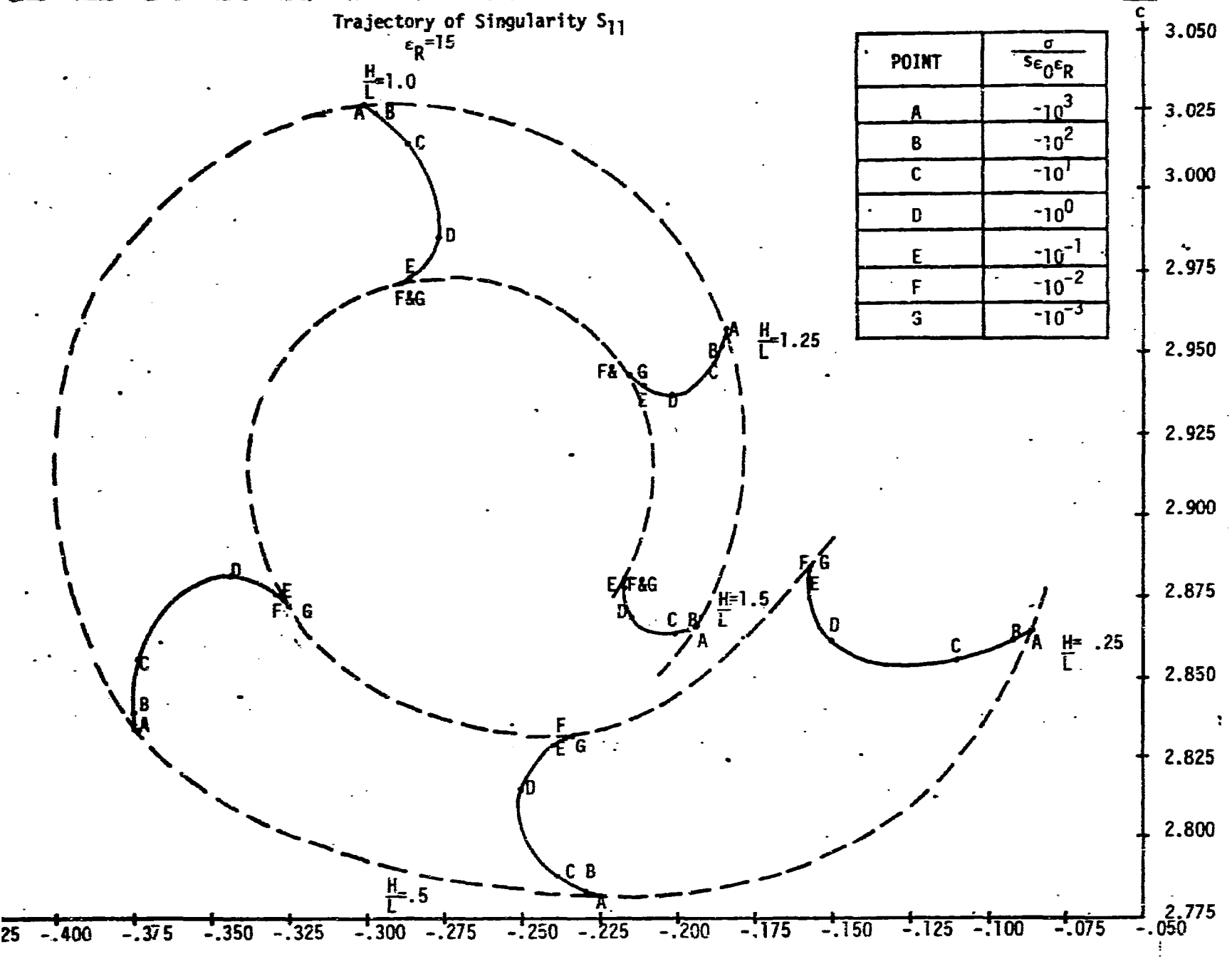

POINT	$\frac{\sigma}{s\epsilon_0\epsilon_R}$
A	-10^3
B	-10^2
C	-10^1
D	-10^0
E	-10^{-1}
F	-10^{-2}
G	-10^{-3}

Fig. 4

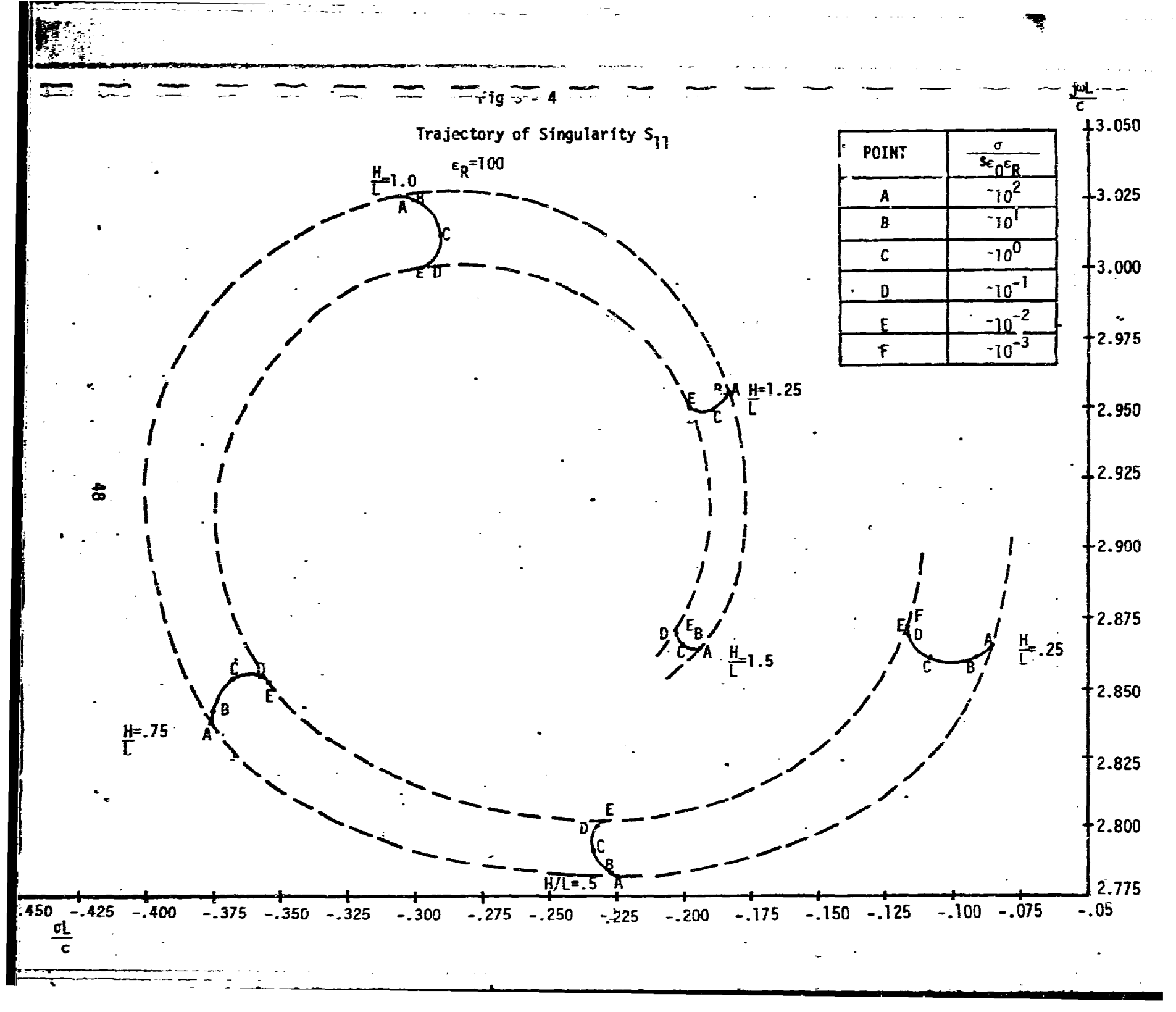
Trajectory of Singularity S_{11}
ϵ_R=100
H/L=1.0
H/L=1.25
H/L=1.5
H/L=.75
H/L=.5
H/L=.25
A
B
C
D
E
F
POINT
$\frac{\sigma}{s\epsilon_0\epsilon_R}$
A -10^2
B -10^1
C -10^0
D -10^{-1}
E -10^{-2}
F -10^{-3}
$\frac{\omega L}{c}$
3.050
3.025
3.000
2.975
2.950
2.925
2.900
2.875
2.850
2.825
2.800
2.775
$\frac{\sigma L}{c}$
-.450
-.425
-.400
-.375
-.350
-.325
-.300
-.275
-.250
-.225
-.200
-.175
-.150
-.125
-.100
-.075
-.05
48

FIG 3

Trajector of Singularity S_{12} $\frac{H}{L} = .6$

$\epsilon_R = 1$

POINT	$\frac{\sigma}{S\epsilon_0\epsilon_R}$
A	-10^4
B	-10^3
C	-10^2
D	-10^1
E	-10^0
F	-10^{-1}
G	-10^{-2}

$\frac{H}{L}=.8$

$\frac{H}{L}=1$

$\frac{H}{L}=.4$

$\frac{H}{L}=.2$

$\frac{j\omega L}{c}$

6.050 6.025 6.000 5.975 5.950 5.925 5.900 5.875 5.850 5.825 5.800 5.775

$\frac{\sigma L}{c}$

-.500 -.475 -.450 -.400 -.375 -.350 -.325 -.300 -.275 -.250 -.225 -.200 .175 -.150

FIG 2 6

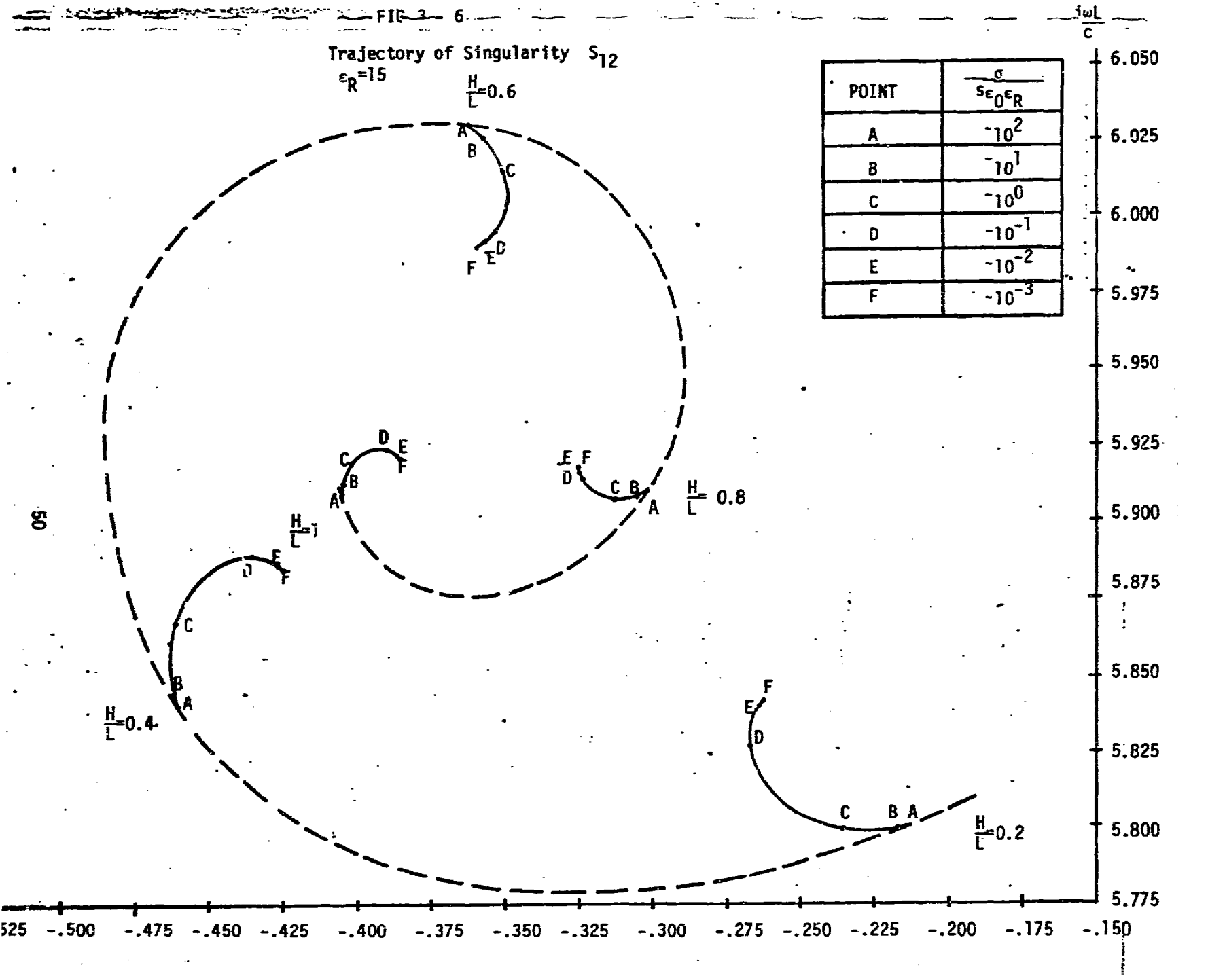

POINT	$\frac{\sigma}{s\varepsilon_0\varepsilon_R}$
A	-10^2
B	-10^1
C	-10^0
D	-10^{-1}
E	-10^{-2}
F	-10^{-3}

FIG 3 - 7

Trajectory of Singularity S_{13}

$\epsilon_R = 1$

POINT	$\frac{\sigma}{s\epsilon_0\epsilon_R}$
A	4793.52
B	479.352
C	47.9352
D	4.79362
E	.479352
F	.0479352
G	.00479352

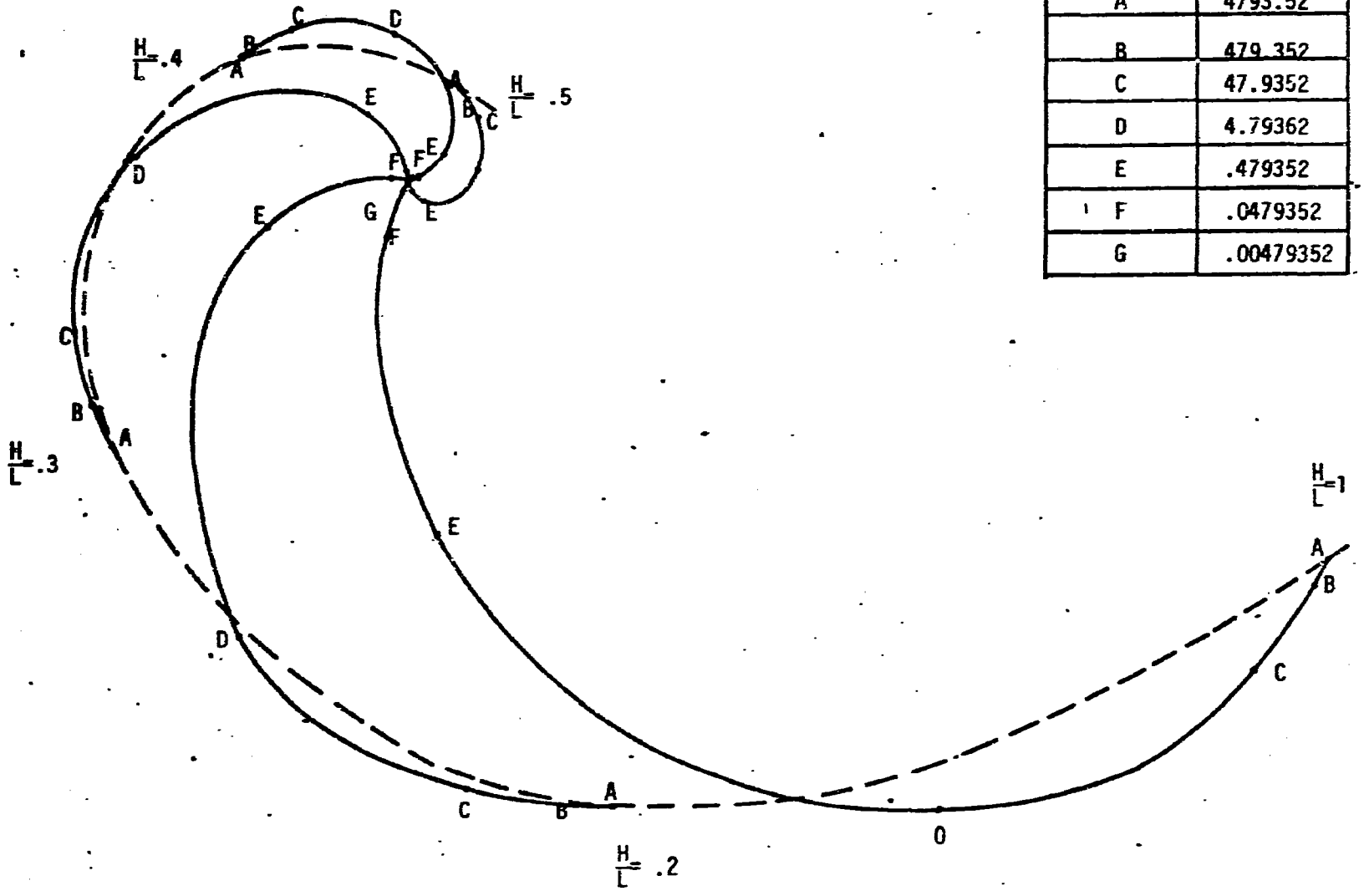

$\frac{j\omega L}{c}$

8.9
8.875
8.85
8.825
8.8
8.775
8.75
8.725
8.7
8.675
8.65
8.625

-.5 -.475 -.45 -.425 -.4 -.375 -.35 -.325 -.3 -.275 -.25 -.225 -.2 -.175 -.15 -.125

$\frac{j\omega L}{c}$

FIG 3 - 8

Trajectory of Singularity S_{13}

$\epsilon_R = 15$

POINT	$\frac{\sigma}{s\epsilon_0\epsilon_R}$
A	319.56
B	31.956
C	3.1956
D	.31956
E	.031956
F	.0031956

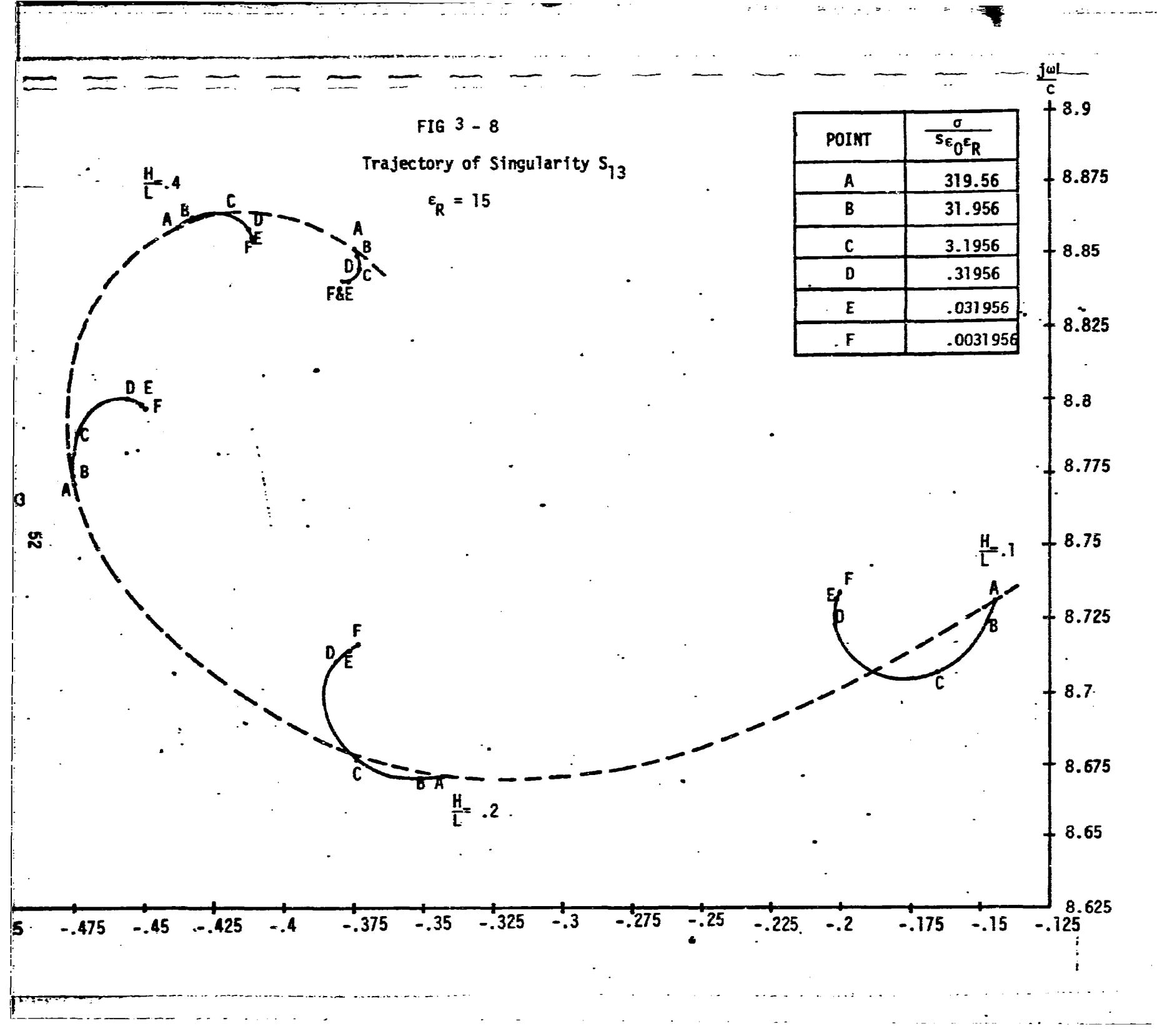

Figure 3-9. Real Part of Normal Mode Vector
Pole S_{11}, ϵ_R=1, $\frac{H}{L}$ = .25, σ=120

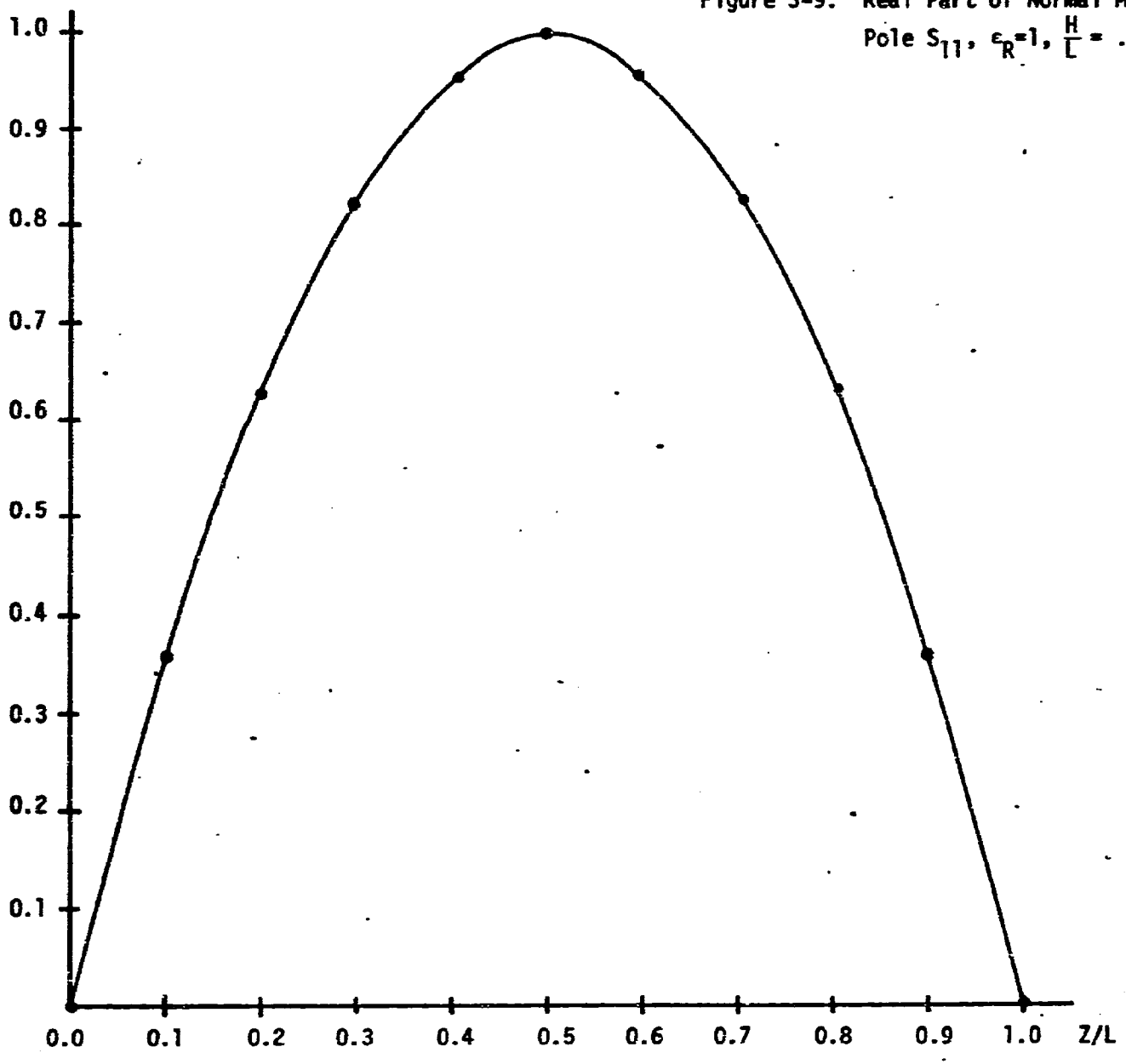

Figure 3-10. Imag. Part of Normal Mode Vector
Pole S_{11}, ϵ_R=1, $\frac{H}{L}$ = .25, σ=120

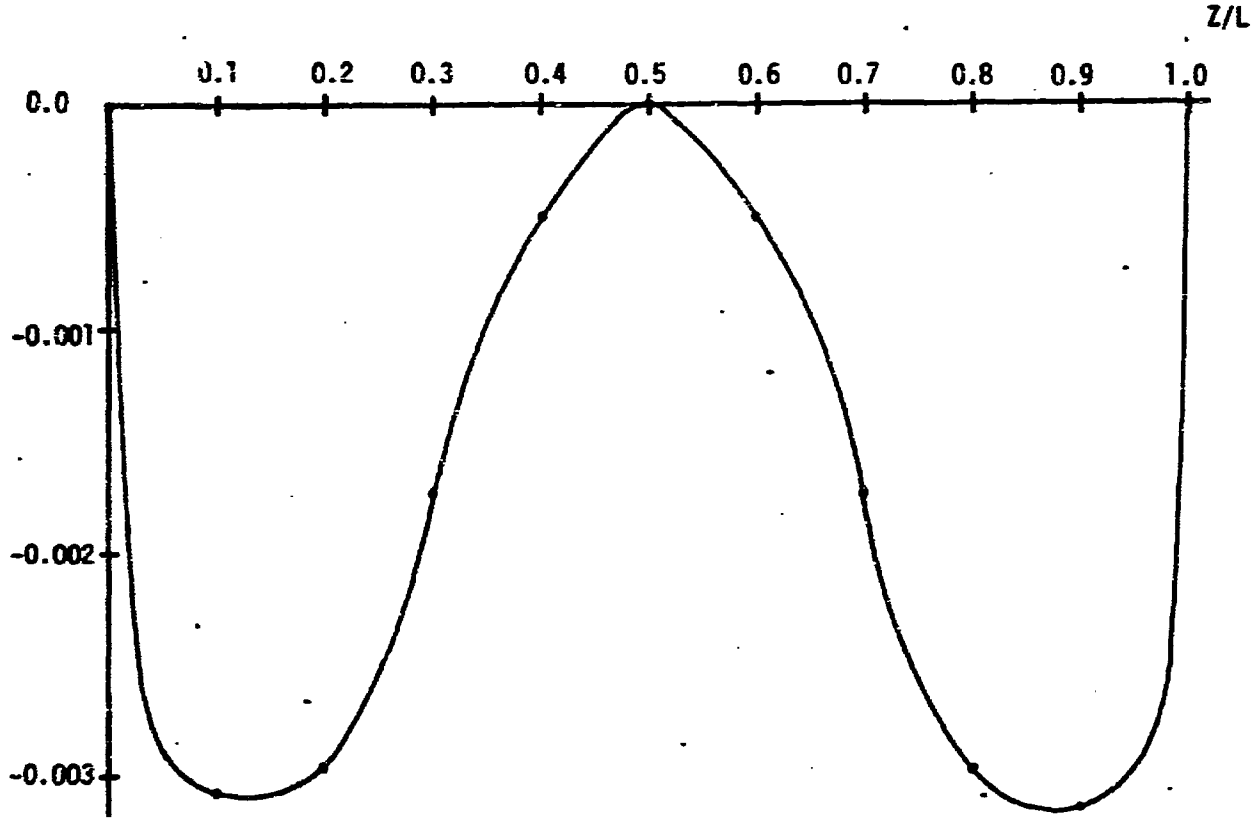

Figure 3-11. Real Part of Normal Mode Vector
Pole S_{12}, ε_R=1, $\frac{H}{L}$ = .2, σ=120

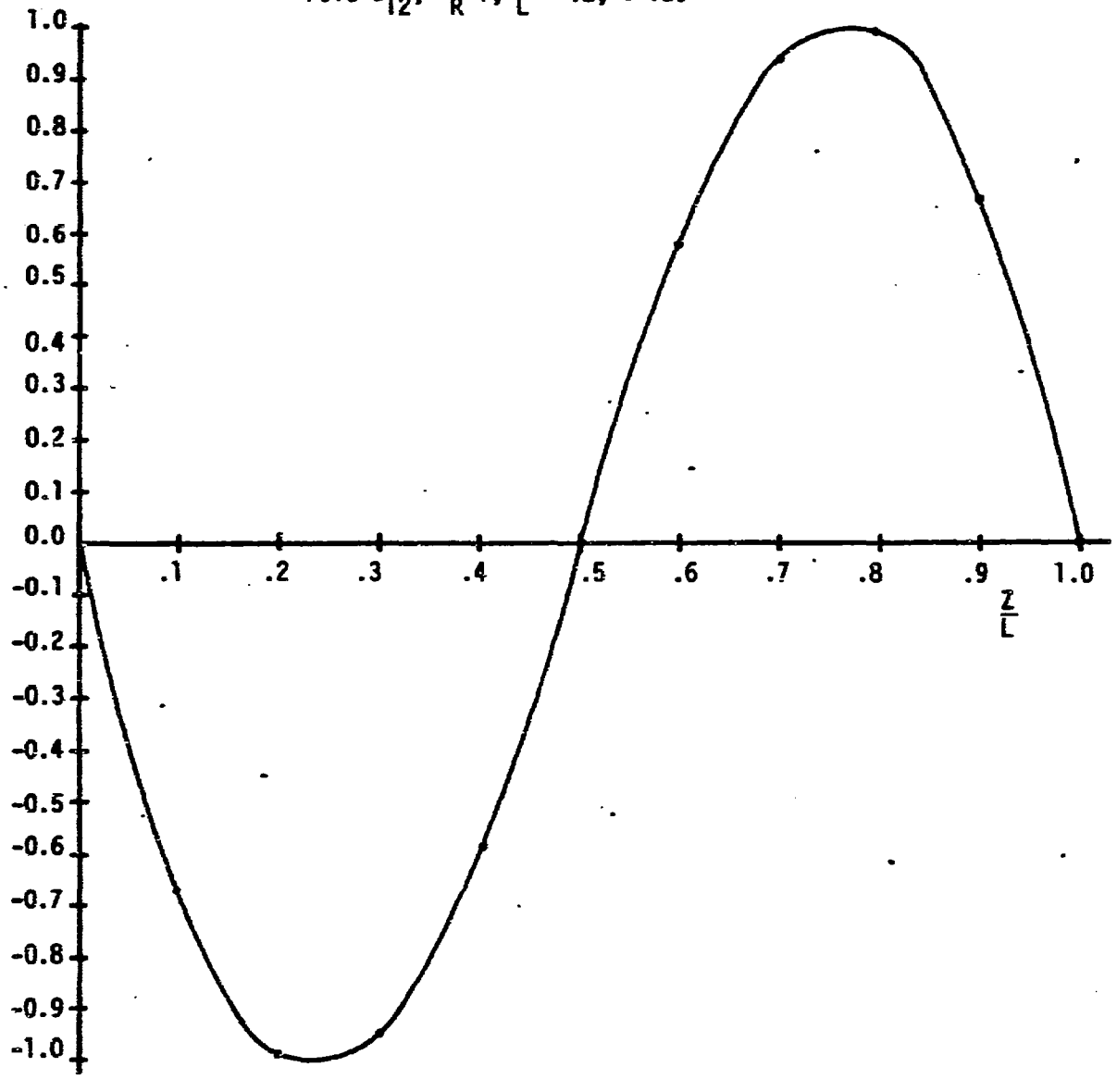

Figure 3-12. Imag. Part of Normal Mode Vector
Pole S_{12}, ε_R=1, $\frac{H}{L}$ = .2, σ=120

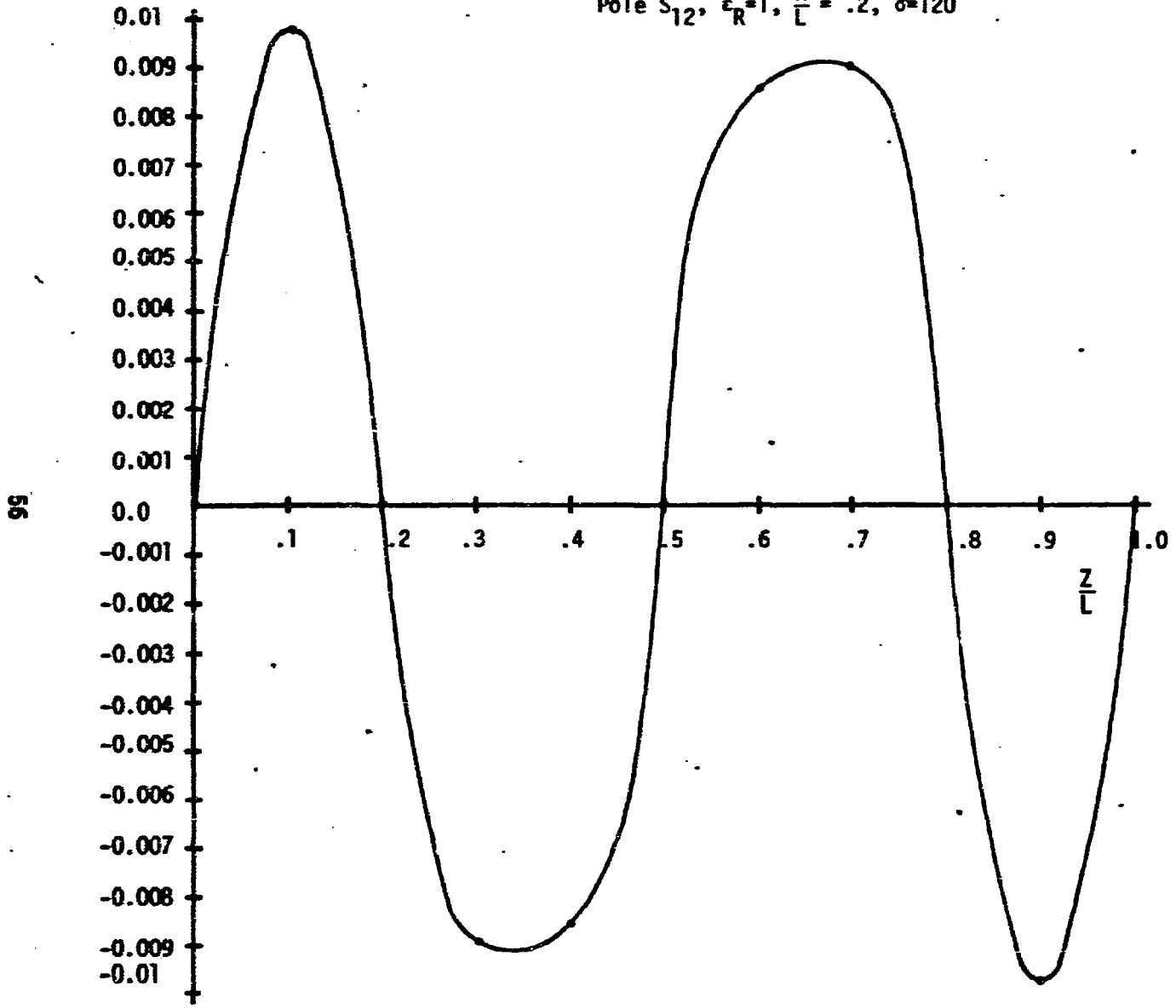

REFERENCES

[1] T. H. Shumpert, "EMP Interaction with a Thin Cylinder Above a Ground Plane Using the Singular Expansion Method," Air Force Weapons Laboratory, Albuquerque, NM, Interaction Note 182, June, 1973.

[2] K. R. Umashankar, "The Calculation of Electromagnetic Transient Currents on Thin Perfectly Conducting Bodies Using the Singularity Expansion Method," Ph.D. Dissertation, University of Mississippi, University, Mississippi, 1974.

[3] K. R. Umashankar, T. H. Shumpert, and D. R. Wilton, "Scattering by a Thin Wire Parallel to a Ground Plane Using the Singularity Expansion Method," IEEE Trans. Antennas Propagat., Vol. AP-23, pp. 178-184, March, 1975.

[4] F. M. Tesche, "On the Behavior of Thin-Wire Antennas and Scatterers Arbitrarily Located Within a Parallel-Plate Region," IEEE Trans. Antennas Propagat. (commun.), Vol. AP-20, pp. 482-486, July, 1972.

[5] Dennis J. Galloway, "Cylindrical Scatterer Near Perfectly Conducting Ground," Master's Thesis, Auburn University, Auburn, Alabama, 1976.

[6] H. J. Schmitt, C. W. Harrison, Jr., and C. S. Williams, Jr., "Calculated and Experimental Response of Thin Cylindrical Antennas to Pulse Excitation," IEEE Trans. Antennas Propagat., Vol. AP-14, pp. 120-127, March, 1966.

[7] J. N. Bombardt, Jr., "Induced Current on a Thin Cylinder Above a Finitely Conducting Half-Space," Harry Diamond Laboratories, Washington, DC, TR-1628, July, 1973.

[8] Robert G. Olsen and David C. Chang, "Current Induced by a Plane Wave on a Thin Infinite Wire Near the Earth," IEEE Trans. Antennas Propagat., Vol. AP-22, pp. 586-589, July, 1974.

[9] Leonard Schlessinger, "Currents Induced by a Plane Wave on an Infinite Wire Above a Flat Earth," IEEE Trans. Electromagnetic Comp., Vol. EMC-17, August, 1975.

[10] T. K. Sarkar and B. J. Strait, "Analysis of Arbitrarily Oriented Thin Wire Antenna Arrays Over Imperfect Ground Planes," Syracuse University, Syracuse, New York, Technical Report TR-75-15, December 1975.

[11] Henry Jasik (Editor), Antenna Engineering Handbook, McGraw-Hill, New York, NY, pp. 2, 6-7, 1961.

[12] F. E. Terman, Electronic and Radio Engineering, McGraw-Hill, New York, NY, pp. 882-886, 1955.

[13] John D. Kraus, Antennas, McGraw-Hill, New York, NY, pp. 303-314, 1950.

[14] E. C. Jordon, Electromagnetic Waves and Radiating Systems, Prentice-Hall, Englewood Cliffs, NJ, 1950.

[15] P. R. Bannister, "The Image Theory Quasi-Static Fields of Antennas Above the Earth's Surface," Navy Underwater Sound Laboratory, New London, Connecticutt, Report No. 1061, December, 1969.

[16] Jery D. McCannon, "Comparative Numerical Study of Several Methods for Analyzing a Vertical Thin-Wire Antenna Over a Lossy Half-Space," Ph.D. Dissertation, University of Illinois at Urbana-Champaign, 1974.

[17] C. D. Taylor, "On the Circumferential Current and Charge Distributions of Circular Cylinders Near a Ground Plane," Air Force Weapons Laboratory, Albuquerque, NM, Interaction Note 138, March 1973.

[18] R. F. Harrington, Time-Harmonic Electromagnetic Fields, McGraw-Hill New York, NY, 1961.

[19] R. F. Harrington, Field Computation By Moment Methods, McMillan Co., New York, NY, pp. 62-81, 1966.

[20] R. Mittra (Editor), Computer Techniques for Electromagnetics, Pergamon Press, New York, NY, 1973.

[21] R. F. Harrington, "Matrix Methods for Fields Problems," Proc. IEEE, Vol. 55, pp. 136-149, February, 1967.

[22] P. C. Waterman, "Matrix Formulation of Electromagnetic Scattering," Proc. IEEE, Vol. 53, pp. 805-812, August, 1965.

[23] Carl E. Baum, "On the Singularity Expansion Method for the Case of First Order Poles," Air Force Weapons Laboratory, Albuquerque, NM, Interaction Note 129, October, 1972.

[24] Carl E. Baum, "Use of Locally Quasi-Static Modes on Thin Structures to Expand the Electromagnetic Response," personal communication, 1975.

[25] Carl E. Baum, "On the Singularity Expansion Method for the Solution of Electromagnetic Interaction Problems," Air Force Weapons Laboratory, Albuquerque, NM, Interaction Note 88, December, 1971.

[26] Lennart Martin, R.W. Latham, "Analytical Properties of the Field Scattered by a Perfect Conducting, Finite Body," Northrop Corporate Labs, Interaction Note 92, Jan. 1972.

[27] Lennart Martin, "Natural-Mode Representation of Transient Scattering from Rotationally Symmetric, Perfectly Conducting Bodies and Numerical Results for a Prolate Spheroid," Northrop Corporate Labs, Interaction Note 119, Sept. 1972.

[28] Lennart Martin, R. W. Latham, "Analytical Properties of the Field Scattered by a Perfect Conducting, Finite Body," Northrop Corporate Labs, Interaction Note 92, Jan. 1972.

[29] F. M. Tesche, "Application of the Singularity Expansion Method to the Analysis of Inpedance Loaded Linear Antennas," Dikewood Corporation, Sensor and Simulation Note 177, May 1973.

[30] F. M. Tesche, "On the Singularity Expansion Method as Applied to Electromagnetic Scattering from Thin Wires," Dikewood Corporation, Interaction Note 102, April 1972.

[31] Olav Einarsson, "A Comparison Between Tube-Shaped and Solid Cylindrical Antennas," IEEE Trans. Antennas Propagat., Vol. Ap-14 pp. 31-37, January 1966.

[32] K. A. Norton, "The Physical Reality of Space and Surface Waves in the Radiation Field of Radio Antennas," Proc. IRE, Vol. 25, pp. 1192-1202, September 1937.